CHAPTER 13

THERMAL TRANSPORT IN POLYMERS

Asegun Henry

George W. Woodruff School of Mechanical Engineering, Georgia Institute of Technology, Atlanta, Georgia 30332; E-mail: ase@gatech.edu

An introduction to polymers and their thermal conductivity is provided, with particular attention paid to recent work that has highlighted the potential to make high thermal conductivity polymers. The thermal conductivity of amorphous polymers is generally low, on the order of 0.1–1.0 W m^{-1} K^{-1}*; however, polymers can be inexpensive to manufacture and they are corrosion resistant and lightweight, which makes them attractive for heat transfer applications. To realize their potential, higher thermal conductivity and higher strength is needed, which can be achieved to some extent by adding fillers to a polymer matrix. A review of the strategies employed to raise the thermal conductivity of polymers is provided along with an introductory review of the physics that intrinsically allows individual polymer molecules to serve as good heat conductors.*

KEY WORDS: *polymers, thermal conductivity, phonon transport, anomalous heat conduction*

1. INTRODUCTION TO POLYMERS

Polymers are materials composed of long molecular chains, in which each chain consists of repeated structural units called monomers. The chemical process of linking monomers together to form chains is termed polymerization, and although there are but a handful of industrially dominant monomers [e.g., ethylene, propylene, vinyl chloride, styrene, etc. (see Fig. 1)], there are thousands of polymers found throughout nature.[1,2] For example, the human body contains many natural polymers such as proteins and nucleic acids, while the structure of plants is primarily comprised of cellulose, the most common organic compound on earth. Polymers can be as short as just a few monomers or as long as tens of thousands of monomers. For example, during synthetic polymerization of ultra-high molecular weight polyethylene (UHMWPE), chains containing $>$1000 monomers can be formed.[1,2] The average chain length is usually denoted by the average weight of each macro-molecule, termed molecular weight (MW), which can affect the material properties such as the modulus and thermal conductivity.

There are three typical definitions[1,2] for a polymer's MW; namely

$$\frac{\sum M_i N_i}{\sum N_i} \tag{1}$$

$$\frac{\sum M_i^2 N_i}{\sum M_i N_i} \tag{2}$$

ISSN: 1049–0787; ISBN: 1–978–56700–295–9/14/$35.00 + $00.00

NOMENCLATURE

a	lattice constant
C	specific heat (J m^{-3} K^{-1})
COP$_T$	coefficient of performance
E	energy (J)
k_B	Boltzmann's constant, 1.3806×10^{-23} J/K
k_E	Einstein coefficient
M	molecular mass
N	number of chains
p	thermal conductivity ratio
Q	heat transfer rate (W)
t_L	lifetime (s)
U	particle interaction energy
W_p	pumping energy (J)
W_m	manufacturing energy (J)
x	particle separation
X	mode amplitude

Greek Symbols

θ	angle (rad)
θ_D	Debye temperature (K)
κ	thermal conductivity (W m^{-1} K^{-1})
κ_e	effective thermal conductivity (W m^{-1} K^{-1})
κ_f	filler thermal conductivity (W m^{-1} K^{-1})
κ_{I}	thermal conductivity due to normal phonon processes (W m^{-1} K^{-1})
κ_{II}	thermal conductivity due to Umklapp phonon processes (W m^{-1} K^{-1})
κ_m	matrix thermal conductivity (W m^{-1} K^{-1})
Λ	mean-free path (m)
λ	wavelength (m)
λ_{DR}	draw ratio
τ	relaxation time (s)
φ	volume fraction
$\varphi_{\max}$	maximum particle packing fraction
ψ	sphericity

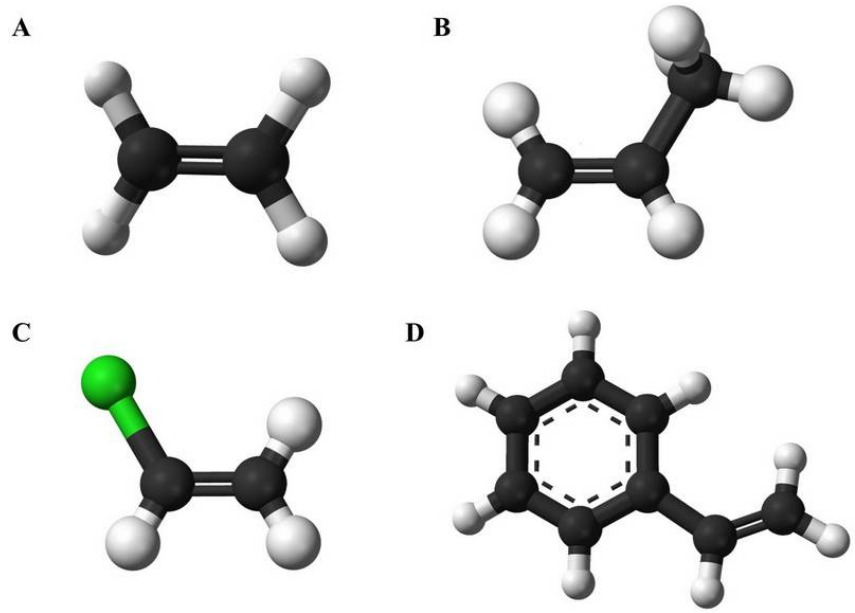

FIG. 1: Four of the most commonly produced monomers: (A) ethylene (C_2H_4); (B) propylene (C_3H_6); (C) vinyl chloride (C_2H_3Cl); (D) styrene C_8H_8.

$$\frac{\sum M_i^3 N_i}{\sum M_i^2 N_i} \tag{3}$$

the number average MW [Eq. (1)], weight average MW [Eq. (2)], and the z-average MW [Eq. (3)]. Here, M_i is the total mass of a chain with i monomers and N_i is the number of chains in the material with that mass. The number average can be predicted by polymerization mechanisms related to the underlying chemistry. The weight average takes into account the weight of a chain in determining its contribution to the weight average, and thus the more massive the chain, the more it contributes to the MW. The z-average and other higher-order averages can be defined by increasing the exponents in the numerator and denominator of Eq. (3), placing greater emphasis on the most massive chains. In practice, the weight average tends to be a more useful definition because it accounts for the contributions of different-sized chains to the overall behavior of the polymer, and therefore correlates best with physical properties.[1,2] The ratio of the weight average to the number average is termed the polydispersity index, and it is often used as an indication of the width of the distribution. Many polymer properties—such as the glass transition temperature, modulus, tensile strength, etc.—increase; however, they eventually plateau with increasing MW. For example, individual monomers tend to have the smallest values of the aforementioned properties, and as the number of monomers increases the properties tend to increase sharply until a plateau is reached. However, other properties that are important for processing, such as the viscosity and solution viscosity, exhibit a strong and continual increase with increasing MW.[1−3] Consequently, there is often an optimal MW that strikes a balance between plateauing performance and increasing energy required for processing.[1,2]

Industrially, polymers are primarily derived from crude oil, natural gas, or other petrochemicals.[4] Monomers are typically synthesized by distilling crude oil to separate its major constituents. The constituents are typically cracked at high temperature (500–1000°C) and low pressure with steam to form monomers such as ethylene, which is the most common.[4] From just a few base monomers, other monomers can be synthesized, or the monomers can be directly polymerized. Most polymers can be classified as either plastics or rubbers. Plastics are usually rigid in their applications and have elastic moduli on the order of 1–10 GPa.[1,2] On the other hand, rubbers can be more flexible, some with moduli below 0.01–0.1 GPa.[1,2] In rubbers, polymer molecules can move and deform easily when stress is applied. Vulcanization is the process of adding elements such as sulfur or other chemicals to form cross-links between the polymer chains; thereby increasing rigidity. This synthetic process allows the properties of rubbers to be tuned for a wide variety of applications ranging from soft and flexible automobile tires or shoe soles to hard and rigid bowling balls.

Plastics can be generally divided into two categories; i.e., thermosets and thermoplastics. Thermoplastics can be reversibly melted and solidified without any change in chemical bonding. Thermoplastics typically become pliable or moldable above a certain temperature and then return to a solid state upon cooling. For example, polyethylene (PE) can be melted, reformed, and solidified into a new shape without changing the chemical bonding. Most thermoplastics have a high MW, and the molecular chains interact through long-range intermolecular forces (i.e., van der Waals or Coulombic).[1,2] This property allows thermoplastics to be remolded because their intermolecular bonds spontaneously reform upon cooling. On the other hand, thermosets such as polymethyl methacrylate (PMMA)

or epoxies are polymers that irreversibly form chemical bonds during the curing process. These new, typically covalent, chemical bonds cross-link the polymer chains, forming a matrix of long chains with interlocking connections.

A major reason for the increasingly widespread usage of polymers for various applications is their light weight, specifically in the context of packaging applications, which is the largest usage of polymers. Plastics by themselves are the third largest industry in the United States; Fig. 2 shows that in the late 1980's the volume production of plastics exceeded that of steel.[5] This is primarily because of the usage of plastics for packaging, where they have proved advantageous over glass or metals (i.e., aluminum) due to their lower weight and, therefore, lower cost for transportation.[5] Polymers can also be slightly permeable to air, which can be advantageous in food preservation. Another reason plastics have become preferred in food packaging applications is that they cannot injure the consumer if they are broken or damaged, which makes them safer to use. In other applications, such as building, construction, and automotive applications, the fact that polymers are generally highly corrosion resistant makes them advantageous over other materials. However, one of the most important advantages of polymers is their associated ease of manufacturing. Polymers can be more cost effective than alternative materials, such as metals, which may have comparable feedstock costs but may have higher final manufacturing costs because of the energy required in forming them. It is in this respect that injection molding of polymers has become a preferred method for shape molding polymers for various applications, due to its low cost.[5,6] Thermoplastics are thus a major part of the polymer industry. Figure 2 also shows that the four highest production polymers constitute ∼84% of the thermoplastics industry.[5] Bulk polymers are also easily machined and their mechanical properties are usually strongly dependent on temperature at moderate temperatures (–100–400°C), which enables a variety of approaches to manufacturing.[2,6]

Plastics and rubbers can be reinforced by other materials to form composites, which allows for an even wider range of possible materials/properties. The intrinsic properties of

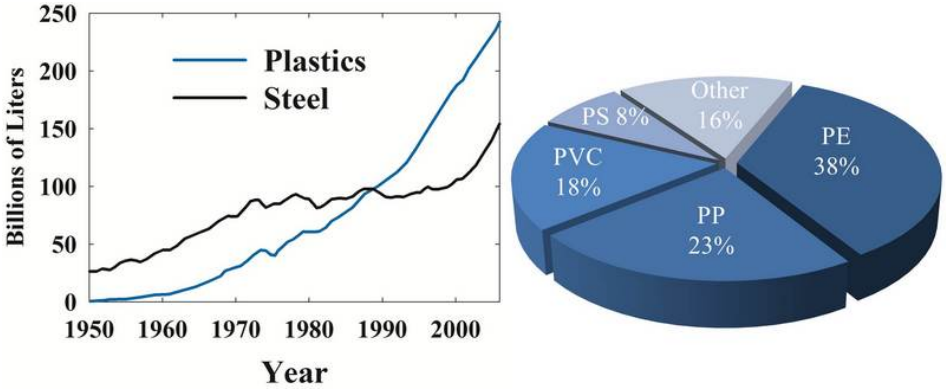

FIG. 2: History of global plastics versus steel production and 2007 market share of global thermoplastics production. (A) In 1989 the production of plastics by volume exceeded that of steel. (B) Thermoplastics global market share, highlighting the four most common polymers: polyethylene (PE), polypropylene (PP), polyvinylchloride (PVC), and polystyrene (PS).

the polymer host can be tuned during chemical synthesis, while fillers and additives can also be added to further tune the properties for specific applications. For example, carbon nanotube (CNT) polymer composites have been studied extensively[7−18] because of the high thermal conductivity of individual CNTs.[19−25] Graphite–polymer composites have also been investigated extensively,[26−32] as well as metal–polymer composites[33−35] and ceramic–polymer composites.[36−44] In most cases, the composite properties resemble that of an effective medium in which the composite property is a weighted average of the constituents. It is in this respect that multicomponent composites have an immense range of attainable properties. As a result, polymers and composites are widely used because they serve an enormous variety of functions, including fibers, monofilaments, textiles, rope, film, membranes, paints, photoresist, adhesives, sealants, foams, containers, moldings, absorbents, fillers, additives, etc. The wide utilization of polymers stems, in part, from the tunability of their properties and the inexpensive processes required to form them into desired shapes.[1,2,5,6]

Another reason for the continual rise in polymer production is the ever increasing number of applications in which they are used. It is in this sense that polymers have even begun to find their way into heat transfer applications, which has prompted their inclusion in this volume. Polymers are generally regarded as thermal insulators with low thermal conductivities on the order of 0.1–1.0 W m^{-1} K^{-1}. However, a major undertaking of the present chapter is to review more recent attention to developments in the synthesis of high thermal conductivity polymers and composites.[7,45−47]

Although most of the tuning of the thermal conductivity of polymers has been achieved with additives, over the last 15 years more attention has been given to the notion of actually changing the intrinsic thermal conductivity of polymers.[45,46,48−52] This idea was initially pioneered by C. L. Choy, starting as far back as the late 1970's.[48,51] The idea is that, in the amorphous phase, polymers are insulators because the molecular chains are entangled. However, when mechanically stretched, the chain alignment increases and heat can flow more efficiently down the polymer backbone (the chain axis). This has a strong effect on thermal conductivity and has been demonstrated by Choy et al.[46,48,49,52] and their coworkers.[51] Most recently, the thermal conductivity of ultra-drawn PE nanofibers was measured, with κ as high as 104 W m^{-1} K^{-1}, which is higher than most elemental metals.[45] Such a high thermal conductivity indicates the possibility that polymers can serve as cheap heat conducting materials, providing competition and alternatives to metals. Although this dramatic increase in the thermal conductivity of PE has been observed as far back as the 1970's,[48,51] to our knowledge a commercial application using high thermal conductivity PE has not been realized. This is likely due to the absence of a scalable manufacturing process to make such a material straightforward to use in existing products or industries; thus, a major challenge in realizing this great potential lies in creating a large-scale manufacturing process that will be attractive to existing or emerging industries.

2. HEAT TRANSFER APPLICATIONS

Polymers are attractive materials as heat exchangers for several reasons. (1) Polymers can be less expensive and require less energy to manufacture than metals. (2) Polymers can be

more corrosion resistant than metals. (3) Polymers are generally lightweight and can be transported and assembled easier than other choices of materials. The drawbacks, which have prevented widespread usage of polymer heat exchangers, include low thermal conductivity, low strength, and low operating temperature. In some cases the disadvantage of low thermal conductivity can be countered by minimizing the wall thickness of the heat transfer surfaces so that the conductive resistance is minimized. In particular, for applications in which the convective heat transfer rate is low (i.e., to a gaseous medium at low flow speeds), it is possible to minimize the thickness to a point where the convective resistance dominates. In these situations, polymers can potentially be more cost effective than metals. However, for many large industrial applications, high thermal conductivity and high strength is still needed. Cevallos et al.[53] provided an excellent review of the history and potential future of polymer-based heat exchangers. The reader is directed to their review[53] for more details, as only a concise summary is provided herein.

As far back as 1965, DuPont[54] was the first to successfully design and manufacture polymer heat exchangers, which consisted of small polytetraflouroethylene [(PTFE) also known as Teflon] tubes that were bundled to form a rigid honeycomb structure. The interest in a polymer heat exchanger stemmed from the need for heat recovery in various corrosive chemical manufacturing environments that involved chemicals such as sulfuric acid, nitric acid, chloride solutions, phosphatizing baths, metasilicates, etc. Heat recovery can reduce energy consumption and ultimately the net operating cost; however, for this benefit to be realized the frequency of heat exchanger replacement must be minimized. Hence, from a levelized cost point of view, polymer heat exchangers can be cost effective because of their longer life, despite their lower performance/thermal conductivity. Specifically, in environments where scaling and fouling introduces additional series thermal resistance, it can be possible to fabricate polymer heat exchangers with thin enough walls such that wall resistance is negligible and the performance becomes comparable to that of metals.

Other successful implementations of polymer heat exchangers involved heat exchange between two gasses (i.e., air), where the convective resistance dominated.[55−57] However, the major advantage polymers potentially offer is corrosion resistance in harsh/fouling environments. Several investigations on polymer corrosion[58,59] have identified Teflon (PTFE), polyphenylene sulfide (PPS), polyvinylidene fluoride (PVDF), and polyetheretherketone (PEEK) as promising candidates that exhibit excellent resistance to chemical attack. Modeling studies indicate that for applications where a convective resistance dominates, polymer heat exchangers can be more cost effective than metals.[53,60] One metric that can be used to gauge the relative cost effectiveness is the heat exchanger coefficient of performance (COP)[53,60]

$$\mathrm{COP}_T = \frac{Q}{W_p + W_m} \tag{4}$$

where Q is the product of the heat transfer rate $\dot{Q}$ and lifetime t_L; W_p is the product of the pumping power and lifetime; and W_m is the energy expenditure required to manufacture the heat exchanger, and therefore serves as a lower bound for the heat exchanger cost. This metric reflects a direct comparison between the energy savings obtained by using a

heat exchanger to the total energy input to create and operate the heat exchanger. Despite the fact that the actual cost of mechanical work is higher than heat, this ratio provides a qualitative measure of the value of using a heat exchanger for a given application. In one example study of a seawater/methane heat exchanger, for use in the offshore liquefaction of natural gas,[60] evaluation of the COP_T showed that corrosion resistant polymers can outperform metals at low flow rates in which the impact of their lower thermal conductivity is less severe (see Fig. 3). The competitiveness of polymers from this viewpoint stems from their lower energy requirements during manufacture W_m, which translates into a lower cost.

From a fundamental point of view, corrosion resistance is in many ways tied to the strength/thermodynamic stability of a material's chemical bonds. The stronger the bonds, the more energetically unfavorable it is to break those bonds toward formation of other compounds. The energy required for manufacture is also tied to the strength of the chemical bonds in a given material because the shaping of materials typically requires breaking bonds to create new surfaces. Thus, one might expect a highly corrosion resistant material to also have high manufacturing energy requirements. This is the case for corrosion resistant metals such as titanium, nickel, chromium, and their alloys. On the other hand, polymers typically involve more than one type of chemical bonding; i.e., strong covalent intramolecular forces and much weaker intermolecular forces. The difference in bond energy can be as large as two orders of magnitude $\sim$1 eV for covalent bonds and $\sim$0.01 eV for van der Waals interactions.[1,2] As a result, polymers can have both high corrosion resistance and low manufacturing energy requirements because the stiff intramolecular bonds

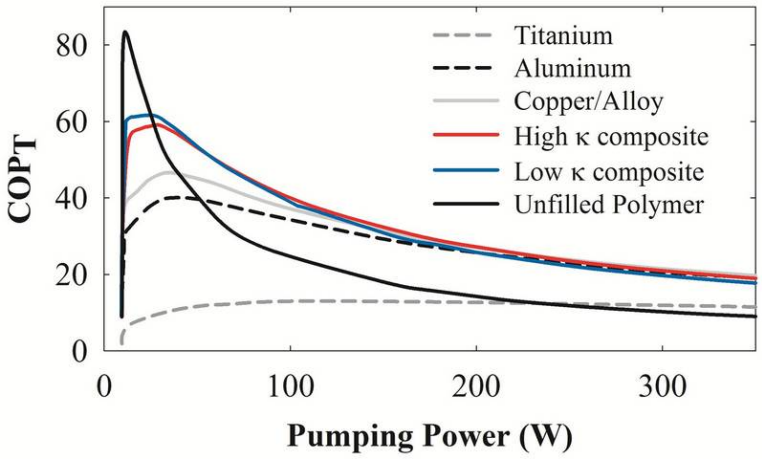

FIG. 3: Coefficient of performance for a seawater/methane parallel-plate heat exchanger made from different materials. The place width and length = 1 m; fin height = 10 mm; fin wall thickness = 1 mm; seawater velocity = 1 m/s; number of fins on the methane side = 100; number of fins on the water side = 5; and heat exchanger lifetime = 1 year. Work required to manufacture: titanium = 1000 MJ/kg; aluminum = 306 MJ/kg; copper/alloy = 72 MJ/kg; high κ composite = 200 MJ/kg; low κ composite = 190 MJ/kg; unfilled polymer = 24 MJ/kg.

provide resistance to chemical attack, while the intermolecular bonds are easily broken during manufacturing. Nonetheless, material strength becomes increasingly important if wall thinning is used as a strategy to overcome the low thermal conductivity of polymers. For this reason, many present day applications continue to employ metals but use a thin coated layer of corrosion resistant polymer for protection. However, the remaining challenge is to somehow raise the thermal conductivity of polymers. To date, that has been primarily done with high thermal conductivity fillers, such as carbon fibers[61−64] and, more recently, CNTs.[7,9,10,12−18] This approach has been successful because commercially available composites exhibit thermal conductivities $\sim$20 W m^{-1} K^{-1}, which is approximately two orders of magnitude higher than the bare polymer matrix. However, a critical parameter in raising the thermal conductivity of a polymer with fillers is the cost of the filler. Since one of the most important advantages of polymers is their low cost, it is important that if a high thermal conductivity composite is developed, the cost remain low. This can be very challenging when considering that high filler fractions (5–50%) are typically needed to observe a major boost in thermal conductivity.[47,65]

Another application for polymer heat exchangers is in the heat recovery of flue gasses with corrosive condensates. Here, polymers are advantageous because of their resistance to chemical attack, but in some cases they are permeable to one or several component species. This can cause swelling and eventual cracking and failure.[53] Nonetheless, there are several applications where polymers are still attractive, such as in salt water desalination evaporators and ocean thermal energy conversion (OTEC),[53,66−69] and as corrosion resistant power plant condensers to enable wastewater cooling and reduce groundwater usage.[70] It is the resistance to the formation of scales and corrosive products that can potentially provide polymers an advantage over metals in the context of non-purified water usage. For example, potential applications could involve the use of seawater for cooling facilities located offshore or near an ocean.

One potentially renewable option for energy conversion is OTEC, which operates via an indirect usage of solar energy. The OTEC concept uses the temperature difference between the surface and deep portions of the ocean to drive a heat engine.[53,66−69] Prototypes used low-pressure Rankine cycles with refrigerants or ammonia as the closed-looped working fluid. The temperature differences in the most favorable locations is $\sim$20–25°C, and thus OTEC cycles only achieve low $\sim$1% efficiencies.[53,66−69] Therefore, the low efficiency requires large surface areas to achieve appreciable power outputs, and the heat exchanger cost and COP$_T$ are expected to be important factors in the system cost effectiveness. The U.S. Department of Energy commissioned research into the development of OTEC systems and identified high-density PE (HDPE) as the material most resistant to corrosion and biofouling.[67,68] However, the low thermal conductivity of HDPE became a limiting factor in the performance and cost effectiveness, since high heat transfer rates can be achieved with liquids, rendering the wall conductive resistance dominant. Research toward the development of OTEC systems terminated shortly after these studies but could be of interest again if major improvements to the thermal conductivity of PE can be achieved.

In addition to large-scale industrial applications, polymers are also used in microelectronics thermal management. In many of today's computers, heat removal from the

processor is critical for performance and reliability. Polydimethylsiloxane (PDMS)-based thermal greases are typically used as thermal interface materials (TIMs) to bond the processor to a metal heat spreader/heat sink.[71,72] These thermosets are deposited in liquid form and cured to form a rigid bond between the package and heat sink. By filling the surface roughness of the chip, they provide good thermal contact and are preferred because of their cost and ease of application, despite their low thermal conductivity $\sim$0.15 W m^{-1} K^{-1}.[73,74] More recently, the idea of using self-assembled monolayers (SAMs) of alkane chains—which are essentially PE chains—to form a thin TIM directly on the package has been explored.[75,76] These studies indicate that the individual chains, covalently bonded to the semiconductor surface using a thiol group, can form high conductance TIMs, where the conductance is likely limited by the thiol group itself.[75,76] Another potential application for polymers in thermal management is in the notion of high thermal conductivity heat spreaders. In this regard, hard plastics, which are typically used as housing and chassis materials, could serve as passive heat spreaders for internal electrical components. At present, these materials primarily serve as mechanical support and protection for the functional components; however, in considering the ever-increasing heat dissipation requirements for various components such as batteries and processors, it may prove advantageous to use the chassis/housing as a heat spreader. This can increase the effective area used for natural convective heat transfer to the surrounding air and can potentially reduce component operation temperatures; thereby increasing lifetime and reliability.

3. AMORPHOUS POLYMER THERMAL CONDUCTIVITY

Most industrial usage of polymers involves materials with some degree of amorphous character. The extremely high aspect ratio of long polymer chains inherently accommodates bends and curvature of the molecules with little resistance or energy penalty. With such a low-energy barrier, configurational entropy drives polymer chains to assume curvilinear shapes, thus forming a highly disordered and entangled amorphous solid structure, often likened to spaghetti. The random orientation and curvature of various sections of a single polymer chain leads to a tortuous path for the propagation of vibrational waves. Atomic vibrational waves, which at low frequencies ($<$100 kHz) are termed sound waves, are typically referred to as phonons in the context of energy transport due to their quantized energy levels.[27,77,78] Phonons in solids are prescribed by plane waves, which can travel linearly through a continuous path of chemically bonded atoms. Phonons/modes of vibration in a polymer chain can interact and exchange energy that, from the phonon (quasi-particle) viewpoint, is described through scattering events. Considering the plane wave nature of phonons, it is intuitive to expect that phonons would be strongly affected by the random curvature and sequence of bends along a polymer chain axis. As a consequence, phonons in amorphous polymers cannot propagate far; typically, less than 10 nm.[79] As such, the thermal conductivity of amorphous polymers generally follows that of glassy/amorphous materials, which has been well described by Klemens.[80] Similar to amorphous glasses, the random curvilinear chain axis leads to structural scattering,[80] and reduces the phonon mean-free path to just a few monomer lengths.[79] Here, the notion of structural scattering implies that as phonons attempt to propagate along the chain and encounter a bend their

propagation is obstructed, leading to a scattering event caused by the polymer structure itself. Thus, the short and effectively constant phonon mean-free path leads to a thermal conductivity, at moderate temperatures, that follows the volumetric specific heat.

Klemens' approach[80] to describing the thermal conductivity of amorphous materials is based on estimating the thermal conductivity contributions from momentum conserving (normal, κ_{I}) and non-momentum conserving (Umklapp, κ_{II}) processes. For most materials, aside from materials with high rates of thermal expansion, phonon velocities exhibit weak temperature dependence (assuming no phase changes), and thus the temperature dependence of the thermal conductivity is mostly governed by the specific heat and relaxation times. For example, based on expressions for the phonon mean-free paths due to normal processes derived by Pomeranchuk[81] and Landau and Rumer[82]

$$\Lambda_L = \frac{Ca}{T}\left(\frac{1}{ak}\right)^4 \tag{5}$$

$$\Lambda_T = \frac{Da}{T^4}\left(\frac{1}{ak}\right), \quad T \ll \theta_D \tag{6}$$

$$\Lambda_T = \frac{D'a}{T}\left(\frac{1}{ak}\right), \quad T \gg \theta_D \tag{7}$$

where the subscript L denotes longitudinal modes; T denotes transverse modes; a is the lattice parameter; k is the wave vector; θ_D denotes the Debye temperature; and C, D, and D' are constants that are usually determined by fitting to experimental data. With these expressions, Klemens[80] estimated the thermal conductivity using the Debye theory of specific heat. At low temperatures the integral over all phonon states reduces to

$$\kappa_{\mathrm{I}}(T) = \frac{3.29AK^2}{3\pi ah}T \tag{8}$$

where K, A, and h are constants that can be determined by fitting to experimental data. At higher temperatures κ_{I} decreases and becomes approximately constant and κ_{II} increases proportional to the specific heat $C(T)$

$$\kappa_{\mathrm{II}}(T) = \frac{1}{3}BavC(T) \tag{9}$$

where B is also a constant that can be determined from experimental data. Klemens[80] estimated the mean-free path by recognizing that it should be proportional to the ratio of the total energy density to the energy density contributed by the relative atomic motion for a specific mode

$$E = \frac{1}{2}\rho q_0^2\left(\frac{2\pi}{\lambda}\right)^2 v^2 \tag{10}$$

$$E_r = \frac{1}{2}\rho q_0^2\left(\frac{2\pi}{\lambda}\right)^4 v^2\Delta x^2 \tag{11}$$

where ρ is the density; q_0 is a constant related to the magnitude of the atomic displacements; λ is the mode wavelength; and Δx is the nearest-neighbor distance. This gives

rise to a constant mean-free path for each mode, even though the constants differ for the transverse and longitudinal polarizations. Using this expression, Klemens[80] was able to describe the low and moderate temperature behaviors of the thermal conductivity of quartz, shown in Fig. 4. Amorphous polymers exhibit the same behavior, where at low temperatures the thermal conductivity is dominated by κ_{I} and transitions to being predominantly dictated by κ_{II} at moderate temperatures. For comparison, Fig. 4 also shows the thermal conductivity of amorphous PMMA and polyethylene terephthalate (PET) as a function of temperature, which is representative of the typical $\kappa(T)$ behavior observed for most amorphous polymers[83] and is well described by Klemens' theory.[80]

To our knowledge, a detailed theory describing polymer thermal conductivity through the glass transition has not been developed. For polymers, the glass transition temperature marks a transition from brittle behavior to a state of high viscosity, where the polymer chains can slide past each other with much greater ease. Morikawa, Tan, and Hashimoto[84] have measured the thermal diffusivity of a number of polymers through their glass transitions. All of the polymers studied exhibit a discontinuity in diffusivity at the glass transition temperature because the chains become more mobile and can slide past each other with greater ease. This subsequently lowers the elastic modulus caused by a weakening in the intermolecular interactions. Intuitively, one would expect that the glass transition then results in lower thermal conductivity because it becomes more difficult for vibrational energy in one chain to couple to surrounding chains and propagate thermal energy in the direction of decreasing temperature. Beyond the glass transition temperature, polymer melts exhibit nearly constant thermal conductivity.[84] The effect of pressure on polymer melts has not been extensively explored, but would not be expected to show strong pressure dependence because polymer melts are well described as incompressible fluids.[83]

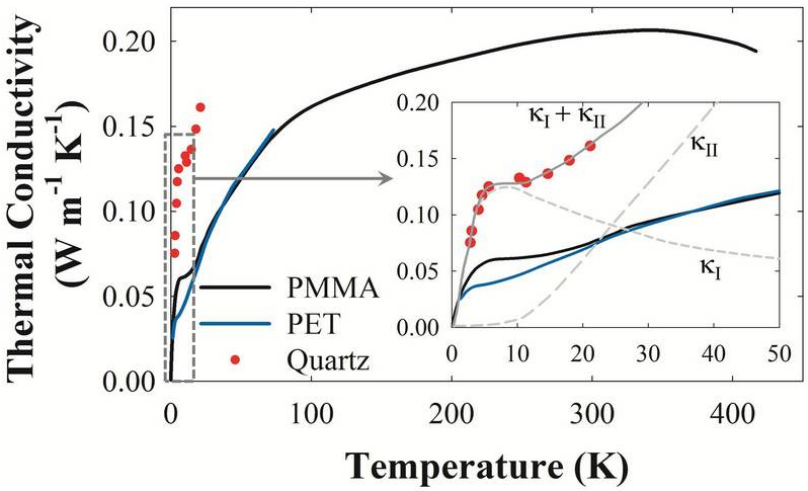

FIG. 4: Thermal conductivity of quartz, amorphous polymethyl methacrylate (PMMA) and polyethylene terephthalate (PET). Inset shows the low-temperature behavior and transition between the dominant contribution from normal and Umklapp phonon scattering. The amorphous polymers show similar behavior to that of quartz glass.

The thermal conductivity of polymers exhibits a dependence on the MW. Phonons are scattered at the chain ends, which is essentially boundary scattering.[79,83,85] As a result, phonons are affected by a combination of parallel scattering processes—namely, intramolecular scattering, intermolecular scattering, structural scattering, and boundary scattering—the combined effect of which can be described with Mathissen's rule as follows:[78]

$$\frac{1}{\tau} = \sum \frac{1}{\tau_i} \tag{12}$$

where τ_i is the relaxation time due to a particular mechanism (i.e., phonon–phonon, boundary, impurity scattering, etc.).

Among the first studies focusing on the MW dependence was that of Ueberreiter and Otto-Laupenmühlen,[86] who measured the thermal conductivity of polystyrene (PS) above and below the glass transition. Their results[86] indicate that thermal conductivity increases with MW, which is likely due to the fact that vibrational energy can propagate along a chain more efficiently than between chains. A theoretical analysis developed by Hansen and Ho[87] suggests that thermal conductivity should increase with the square root of the MW for low MWs and should become approximately constant for high MWs. This theory is in good agreement with experiments,[86−88] examples of which are shown in Fig. 5. However, Hansen and Ho's analysis[87] does not quantitatively predict the range of N, where the thermal conductivity changes most significantly. Nonetheless, their model conceptually suggests that the thermal conductivity is affected by the linear extent of the molecules, which implies that branching should reduce the thermal conductivity for a constant MW. This is qualitatively supported by Tomlinson, Kline, and Sauer,[89] as well as Hennig, Knappe, and Lohe,[90] who measured lower conductivities for branched PE rather than for linear PE.

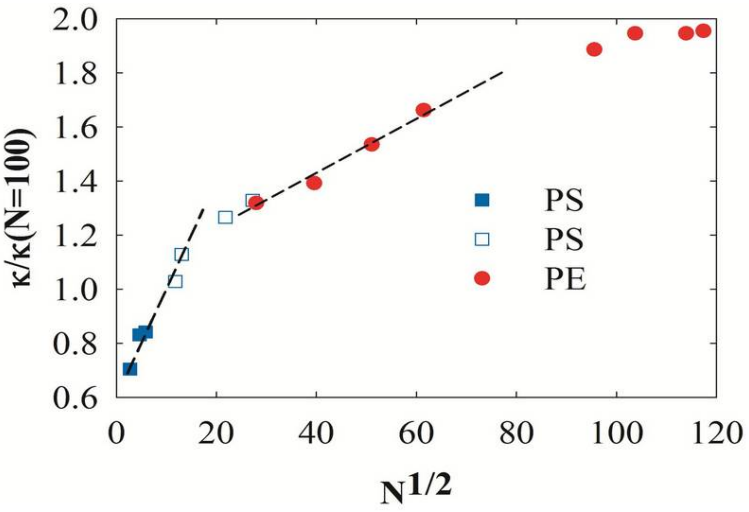

FIG. 5: Thermal conductivity of PS and molten PE versus the average number of monomers in each chain N (proportional to the MW). The thermal conductivity increases with the square root of the chain length at moderate chain lengths and eventually converges to a constant value.

The thermal conductivity of amorphous polymers is generally low, ranging from 0.1 to 1.0 W m^{-1} K^{-1}, and thus they are typically regarded as thermal insulators.[79,83,85] A typical strategy employed to engineer thermally insulating materials is to introduce some form of disorder,[80] weak chemical bonding,[91] anharmonicity/bond strength inhomogeneity,[92,93] imperfections,[94] or interface density.[95] Past efforts utilizing these mechanisms for a variety of applications have been quite successful. On the other hand, engineering high thermal conductivity materials appears to be more challenging, even though the basic mechanisms are well known (i.e., increase bond stiffness, increase long-range order, or minimize the presence of boundaries and interfaces). As previously discussed, the most promising applications for polymers require high thermal conductivity. Thus, a major thrust of past and current research is to find ways to engineer high thermal conductivity polymer-based materials, while keeping in mind that a low-cost solution is likely to have the most commercial value.

4. THERMAL CONDUCTIVITY OF POLYMER COMPOSITES

Most research on engineering polymer thermal conductivity has focused on the use of high thermal conductivity fillers added to low-cost amorphous polymer matrices.[9,12,33,47,63,64] With the low-cost polymer as a matrix/host material, the composite can often be formed into shapes using the same low-cost, high-volume manufacturing techniques currently employed in industry (i.e., extrusion, injection molding, etc.), leading to a low-cost final product with higher thermal conductivity than the original polymer. This composite approach works because the regions occupied by the filler are much more efficient at transporting heat than the polymer itself, leading to a composite thermal conductivity that is some form of a weighted average of the two components' thermal conductivities. In general, the effective composite thermal conductivity κ_e depends on the matrix thermal conductivity κ_m; filler thermal conductivity κ_f; thermal interface resistance (TIR), R, between the filler and matrix; filler particle loading level; as well as the particle shape, size, and dispersion.

Various effective medium (weighted average) models have been developed with varying success at describing experimental data.[96,97] The simplest effective medium theory (EMT) was proposed by J. C. Maxwell Garnett (MG) in 1904,[98] in the context of understanding the optical properties of a glass matrix containing metal spheres dispersed at low enough concentrations such that they have no interaction. This EMT is general and can be applied to thermal conductivity for a two-component system resulting in the following expression for randomly dispersed spheres:[98]

$$\kappa_e = \kappa_m \left[\frac{(p+2) + (p-1)\,2\phi}{(p+2) - (p-1)\,\phi} \right] \tag{13}$$

where φ is the volume fraction and p is the thermal conductivity ratio κ_f/κ_m. This model fits well with experimental data for dilute and randomly distributed components included in a homogeneous host medium, where the particles are isolated with no interactions. However, significant deviations from MG-EMT can occur if the filler volume fraction is high, if the particles have a large aspect ratio, if there is a significant amount of TIR between the

filler and matrix, or if there is any interaction between filler particles. A variety of other models have been derived using different assumptions about the filler and its dispersion and distribution. For example, Donea[99] used variational principles to determine upper κ^+ and lower κ^- bounding effective thermal conductivities for composites with spheres

$$\hat{\kappa} = \kappa_m \left[\frac{(p+2) + (p-1)\,2s}{(p+2) - (p-1)\,s} \right] \tag{14}$$

$$\kappa^- = \frac{\hat{\kappa} \cdot \kappa_m}{\kappa_m + (1-\phi)\,\hat{\kappa}} \tag{15}$$

$$\kappa^+ = \phi\kappa^- + (1-\phi)\,\kappa_m \tag{16}$$

$$s = \left(\frac{a_{\text{in}}}{b} \right)^3 \tag{17}$$

Here, a_{in} is the radius of inclusion and b is the largest possible spherical shell that surrounds the inclusion of random spheres. Donea[99] also used the same procedure to derive an expression for a composite of parallel circular fibers

$$\hat{\kappa} = \kappa_m \left[\frac{(p+1) + (p-1)\,s}{(p+1) - (p-1)\,s} \right] \tag{18}$$

The MG[98] and Donea[99] models were derived for two-component mixtures. Hamilton and Crosser[100] also developed a model for multicomponent composite mixtures, which depends on the sphericity of the filler particles ψ

$$\kappa_e = \kappa_m \left\{ \left[1 - \sum_{i=1}^{N} \frac{\phi_i\,(n_i - 1) \cdot (\kappa_m - \kappa_i)}{\kappa_i + (n_i - 1)\,\kappa_i} \right] \Bigg/ \left[1 + \sum_{i=1}^{N} \frac{\phi_i\,(\kappa_m - \kappa_i)}{\kappa_i + (n_i - 1)\,\kappa_i} \right] \right\} \tag{19}$$

$$n = \frac{3}{\psi} \tag{20}$$

where ψ is the sphericity, defined as the ratio of the surface area of a sphere having equal volume to the particles and the surface area of the particles. Since a sphere has the lowest surface-area-to-volume ratio of any shape, ψ varies between 0 and 1. Initially, for polymer composites, a substantial discrepancy between EMT models and the results of experiments was observed, particularly for polymers with CNTs as fillers. In many of these efforts, the effective thermal conductivity of a CNT–polymer composite was well below that of the EMT predictions because major gains were expected from the fact that CNTs have such a high thermal conductivity. It was later determined that the TIR between the CNT and polymer matrix was a dominant resistance that limited the composite performance. As a result, efforts to lower the TIR and find pairs of polymer matrices and high thermal conductivity fillers that intrinsically have low TIR has become a major focus.[13,44,97] Modified EMT models that account for the TIR between the matrix and filler have also been developed, which correspond better with experimental data.[97] For example, Lin, Zhang, and Wong[101] developed an EMT model for a graphite nanoplatelet–epoxy composite

$$\kappa_{e11} = \kappa_{e22} = \kappa_m \frac{2 + \phi\left[\beta_{11}\left(1 - L_{11}\right)\left(1 + \left\langle\cos^2\theta\right\rangle\right) + \beta_{33}\left(1 - L_{33}\right)\left(1 - \left\langle\cos^2\theta\right\rangle\right)\right]}{2 - \phi\left[\beta_{11}L_{11}\left(1 + \left\langle\cos^2\theta\right\rangle\right) + \beta_{33}L_{33}\left(1 - \left\langle\cos^2\theta\right\rangle\right)\right]} \tag{21}$$

$$\kappa_{e33} = \kappa_m \frac{1 + \phi\left[\beta_{11}\left(1 - L_{11}\right)\left(1 + \left\langle\cos^2\theta\right\rangle\right) + \beta_{33}\left(1 - L_{33}\right)\left(1 - \left\langle\cos^2\theta\right\rangle\right)\right]}{1 - \phi\left[\beta_{11}L_{11}\left(1 + \left\langle\cos^2\theta\right\rangle\right) + \beta_{33}L_{33}\left(1 - \left\langle\cos^2\theta\right\rangle\right)\right]} \tag{22}$$

$$\beta_{ii} = \frac{\kappa_{fii} - \kappa_m}{\kappa_m + L_{ii}\left(\kappa_{fii} - \kappa_m\right)} \tag{23}$$

$$L_{11} = L_{22} = \frac{p^2}{2\left(p^2 - 1\right)} + \frac{p}{2\left(1 - p^2\right)^{3/2}}\cos^{-1}p \tag{24}$$

$$L_{33} = 1 - 2L_{11} \tag{25}$$

$$\kappa_{ef} = \frac{L}{2R + \left(L/\kappa_f\right)} \tag{26}$$

where $\cos\theta$ represents the average orientation of the graphite nanoplatelets and varies between 1 and 3 for random orientations to 1 for completely oriented. Here, the effect of TIR is incorporated with the filler thermal conductivity and serves to reduce its effective thermal conductivity within the matrix. Their study[101] showed that even though their graphite filler had lower thermal conductivity than CNTs, the composite thermal conductivity was higher because of the lower TIR between the graphite and epoxy compared to the CNTs and epoxy. This has been attributed to the smaller diameter of CNTs, which consequently offers little area for interaction and heat transfer to/from the matrix.[13,101] Determining the intrinsic TIR between dissimilar materials/structures remains a significant challenge, but various computational approaches are currently under development.[71,72] Figure 6 shows how the TIR affects the composite thermal conductivity, using Lin, Zhang, and Wong's model.[101] This plot shows how important the intrinsic matrix thermal conductivity is to the composite performance. For example, when the matrix thermal conductivity is raised an order of magnitude from 0.1 to 1.0 W m^{-1} K^{-1}, the rate of increase with filler content changes.

A number of other EMT models have been developed with moderate success to account for the effects of TIR, percolation, and other variations.[13,97,101] However, despite the lack of quantitative agreement in some cases, the models qualitatively capture the main trends. For example, the models generally show that as the volume fraction of a high thermal conductivity filler increases the composite thermal conductivity monotonically increases. However, an exception to this trend would occur if the matrix initially has higher thermal conductivity than the effective thermal conductivity of the filler once the TIR has been incorporated. Adding TIR generally tends to decrease the degree of enhancement, and the percolation effects between filler particles tend to increase composite thermal conductivity. Another general trend is that as p, the ratio of κ_f/κ_m, increases beyond 100, there is diminishing return in the composite enhancement relative to κ_m. For example, Nielson[65] has shown, for spherical particles with a packing fraction of 0.637, that when p is increased beyond 100 there is marginal gain (see Fig. 7). This is because the matrix adds

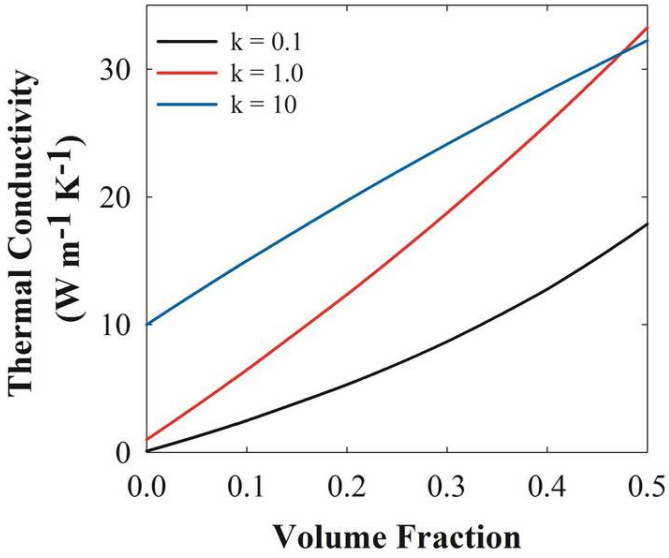

FIG. 6: Graphite nanoplatelet–polymer composite thermal conductivity model predictions. This calculation assumes the thermal interface resistance between the platelets and polymer matrix is 10^{-8} m^2·K/W. As the polymer matrix thermal conductivity is increased from 0.1–1.0 to 10 W m^{-1} K^{-1}, the effect of the high thermal conductivity filler is changed.

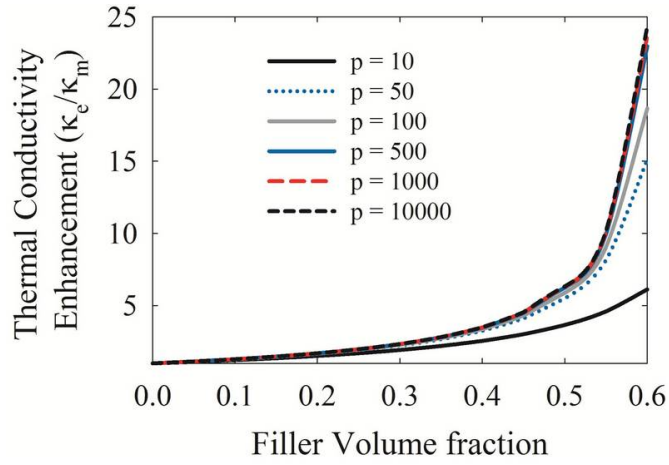

FIG. 7: Theoretical prediction of the relative thermal conductivity enhancement for composites (κ_e/κ_m). The ratio of the filler thermal conductivity (κ_f) to that of the matrix (κ_m) is given by $p - \kappa_f/\kappa_m$.

series resistance to the composite, thus placing an upper limit on the composite thermal conductivity, even in the limit of infinite p. Using Nielson's model[65]

$$\kappa_e = \kappa_m \frac{1 + AB\phi}{1 - B\psi\phi} \tag{27}$$

$$A = k_E - 1 \tag{28}$$

$$B = \frac{p-1}{p+A} \tag{29}$$

$$\psi = 1 + \phi \left(\frac{1 - \phi_{\max}}{\phi_{\max}^2} \right) \tag{30}$$

where A is a constant that depends on the particle shape and orientation with respect to the direction of heat flow, which is related to the generalized Einstein coefficient k_E; B accounts for the relative conductivity between the filler and matrix; and ψ is a factor set by $\varphi_{\max}$, the maximum packing fraction of the filler particles. For rigid spherical particles k_E = 2.5, which leads to A = 1.5. When plotted (see Fig. 7), Eqs. (27)–(30) show that the maximum thermal conductivity enhancement at 50% volume fraction for filler with infinite thermal conductivity is $<$10. Beyond 50%, the high thermal conductivity filler effectively becomes the host matrix, since it comprises the majority of the material. This is an important result because it shows an intrinsic limitation of composites, even in the limit of fillers with infinite thermal conductivity.

The thermal conductivity of polymer composites has been studied extensively, using a range of polymers from PE[16,61] to epoxy[10,11,26,28,38,44] to conjugated polymers such as poly(p-phenylenevinylene-co-2,5-dioctyloxy-m-phenylenevinylene) (PMPV).[102] Filler materials have ranged from oxides to nitrides to carbides and carbon nanostructures such as carbon fiber, CNTs, and graphite nanoplatelets (GnP). The choice of filler and matrix depends on the application constraints. For example, in the context of electronics thermal management it is often desirable to have high thermal conductivity, while maintaining electrically insulating characteristics.[47] For situations in which high electrical resistivity is necessary, oxide fillers such as alumina (Al_2O_3), silica (SiO_2), and zinc oxide (ZnO) have been used.[47] Nitride fillers, such as AlN, Si_3N_4, or BN can have much higher thermal conductivity and SiC has also been used.[47] Some of the aforementioned fillers that have the lowest thermal conductivities, which are still about 1–2 orders of magnitude higher than the amorphous polymers themselves (i.e., silica and alumina), are among the least expensive. Considering Nielson's conclusion,[65] one would expect that choosing a filler with substantially higher thermal conductivity (i.e., 3–4 orders of magnitude higher than κ_m) may not result in much larger enhancement. Nonetheless, considerable research effort has focused on the use of carbon-based materials, which can have thermal conductivities $>$1000 W m^{-1} K^{-1}.[8,9,11,16,17,28,30] For example, CNT polymer composites have received considerable attention[9] because the thermal conductivity of individual CNTs can be $>$2000 W m^{-1} K^{-1},[20–22,24,103] which approaches that of diamond—the highest thermal conductivity bulk material.[104] Synthesis of CNTs is considerably cheaper than diamond, which serves as motivation, but the enhancement of the matrix thermal conductivity is less than one might expect because of the high TIR between the CNTs and matrix. This brings to light an inherent problem with the use of fillers because engineering high thermal conductivity composites can be limited more so by the TIR than the intrinsic filler thermal conductivity.

Considering the issue of TIR between the filler and matrix for composites in which the filler is dispersed in the host material, it remains a difficult challenge to engineer

composites with much higher thermal conductivity than $\sim$ 10–20 W m^{-1} K^{-1}. Although 10–20 W m^{-1} K^{-1} is attractive for certain applications, there is potential to replace metals in many applications, if κ_e can reach 50–200 W m^{-1} K^{-1} inexpensively. An alternative way to increase κ_e is to consider methods to increase the intrinsic thermal conductivity of the matrix κ_m. Using Lin, Zhang, and Wong's model,[101] Fig. 6 shows that raising the matrix thermal conductivity can have a major impact on the composite thermal conductivity. The TIR still plays a critical role; however, Fig. 6 indicates the possibility for a regime of much higher thermal conductivity $>$ 20 W m^{-1} K^{-1}, if κ_m can be increased by an order of magnitude from 0.1 to 1.0 W m^{-1} K^{-1}.

5. THERMAL CONDUCTIVITY OF INDIVIDUAL POLYMER CHAINS

In the pursuit of high thermal conductivity polymers, most research has focused on the development of composites. In particular, the use of carbon-based structures such as carbon fiber, CNTs, and graphite has been studied in detail because of the fact that these fillers can have thermal conductivities on the order of 1000 W m^{-1} K^{-1}.[21,25,105] This regime of high thermal conductivity at room temperature is higher than any metals and is peculiar to carbon-containing materials. In light of this unique quality of carbon-based structures, it is important to consider its physical origin. For such structures the thermal conductivity is dominated by the contribution from phonons (quantized lattice waves in crystals). The thermal conductivity that arises from phonons is proportional to the summed product of each mode's specific heat C, velocity v, and relaxation time τ,[77,78,106]

$$\kappa \propto \sum Cv^2\tau \tag{31}$$

Considering that the specific heat of any mode in any material is, at most, on the order of Boltzmann's constant k_B, this relation shows that the great disparity in room-temperature phonon conductivity for different crystals ($\sim$1–1000 W m^{-1} K^{-1}) is more likely due to the variation in velocity and relaxation times for different materials. Qualitatively, it is also evident from this relation that because thermal conductivity exhibits quadratic dependence on velocity and only linear dependence on relaxation time, one would expect the velocity to show a stronger influence. Additionally, phonon velocities are intrinsically related to elastic moduli, which vary by more than an order of magnitude for different materials. Considering that carbon–carbon bonds are among the stiffest in all of nature, leading to the highest phonon velocities, it becomes clear why carbon-based materials exhibit the highest thermal conductivities. The highest thermal conductivities observed in nature arise in materials with the highest phonon group velocities, which can exceed 15,000 m/s in carbon-based materials.[107,108]

Considering this as the physical origin of their high thermal conductivity, it is also interesting to note that most polymers themselves contain carbon–carbon bonds, and therefore have the potential to transmit the energy of phonons at high speeds. This intrinsic characteristic of polymers that have carbon backbones, such as PE, polyacetalene (PA), polyvinyl chloride (PVC), Teflon, etc., can potentially give rise to very high thermal conductivities for individual chains, since phonons can propagate at high speeds. In the amorphous phase, this potential for efficient heat conduction is hampered by the disordered arrangement of

the chains. Thus, phonons are unable to propagate for a large distance in a straight unimpeded line. Instead, when the chain curves to a different direction the phonons are efficiently scattered, which results in a drastic reduction in τ compared to a single elongated chain. The dominant mode of heat conduction then becomes the transmission of vibrational energy between chains because that becomes the path of least thermal resistance. As a result, the possibility of intrinsically high thermal conductivity for polymers may only exist for elongated single molecules or arrays of aligned chains.[109]

Direct measurement of the thermal conductivity of individual polymer chains is challenging,[109] and therefore much of the work done at the single molecule level has relied on atomistic level modeling. Molecular dynamics (MD) simulations[93,107,108] and measurements of aligned chains[48,49,51,52] and nanofibers[45] all suggest that individual chains do exhibit very high thermal conductivity. In fact, MD simulations predict that the thermal conductivity of individual polymer chains can actually diverge in the limit of an infinitely long chain.[107,108] This phenomenon of divergent thermal conductivity is linked to the discovery of non-ergodic behavior in hypothetical one-dimensional (1D) lattices with nonlinear interactions, first observed by Fermi, Pasta and Ulam (FPU) in the 1950's.[110] A great body of research in nonlinear dynamics has been devoted to understanding the conditions necessary for such anomalous behavior in the simplest possible hypothetical systems; i.e., toy models.[111−132] Here, it is important to note that one dimensionality need only be associated with the periodicity of the structure because the motions of the particles can be in three dimensions and still show divergent behavior.

It is well known that in the limit of perfectly harmonic interactions (quadratic potential $\rightarrow$ linear forces) for the particles in a 1D chain, each normal mode of vibration is orthogonal to all others and the vibrations of the particles can be solved analytically by a superposition of normal modes with constant amplitudes. In this limit, the modes are non-interacting because the initial partitioning of their energy remains constant in time. However, when some degree of nonlinearity is introduced, in many cases analytical solutions become intractable and only numerical solutions can be used to determine the particle trajectory. The most common viewpoint in understanding the behavior of such nonlinear systems is to describe the particle trajectories as a superposition of the solutions to the linear problem; however, instead of constant amplitudes the nonlinearity introduces time dependence in the modal amplitudes. As such, the modes of a nonlinear system interact and exchange energy between them, which from the phonon quasi-particle perspective is represented as scattering events. Thus, from a thermal perspective, perfectly harmonic interactions lead to infinite thermal conductivity because the modes never scatter $\tau \rightarrow \infty$. On the other hand, with nonlinear interactions the modes do interact/scatter, and assuming the scattering events are random (uncorrelated in time) the nonlinearity should lead to an equipartitioning of the modal energy. Equipartition of the mode energy implies that the trajectory is ergodic, and thus nonlinear systems exhibit finite thermal conductivity. The unexpected result from the FPU study[110] was that they observed non-ergodic behavior for a chain of oscillators with nonlinear interactions. The nonlinearity causes the modes to interact, as expected, but at sufficiently long times such that the trajectory repeats itself, which demonstrates that the modal interactions are not random but indeed correlated in time.

This effect appears to be a consequence of one-dimensionality in the particle periodicity and essentially suggests that even in a chain with nonlinear interactions, divergent thermal conductivity is possible. Here, it is important to draw the distinction between this phenomenon, which we will term anomalous heat conduction, and the length-dependent, yet convergent, thermal conductivity of various materials and structures. A number of MD simulations have indicated that the thermal conductivity of CNTs, for example, increases with their length.[132−136] This length dependence arises from ballistic heat conduction for a number of acoustic modes and is well described by expressions derived from the Boltzmann equation. The idea is simply that at nanometer length scales the mean-free path, $\Lambda = v\tau$, of some phonons is longer than the CNT length. Therefore, these phonons can propagate the length of the entire CNT and only scatter at its ends. Thus, as the CNT length is increased the phonon mean-free paths increase, leading to higher thermal conductivity. A number of studies have shown this increasing trend[132−136] in thermal conductivity, which inherently suggests that the thermal conductivity may diverge as $L \to \infty$. However, Mingo and Broido have shown that this is not the case.[23] At sufficient lengths (>10 μm), the boundary scattering at the CNT ends—which limits the thermal conductivity at smaller length scales—is eventually overcome by phonon–phonon scattering. As a result, the thermal conductivity converges to a very high, yet finite, value.[23] The key distinction between this behavior and anomalous heat conduction[107,108] is that for a non-ergodic chain the thermal conductivity would not converge at any length scale. This means that an infinitely long chain could have infinite thermal conductivity.

The relevance of this discussion with respect to polymers is based on recent MD simulation results,[107,108] which showed that even a real model of a polymer chain can exhibit anomalous heat conduction. Previously, such studies[111−130,137] were focused on hypothetical toy models to elucidate the underlying physics. There are three prominent approaches used to study this phenomenon;[138] namely, the mode coupling theory,[139,140] the renormalization group theory,[141] and the Boltzmann equation.[128] The focus of these approaches is to determine how the thermal conductivity diverges with the system size. The usual procedure is to truncate the ∞ upper limit of the integration of the heat flux autocorrelation $\langle Q(t) \cdot Q(t+t') \rangle$ in the Green–Kubo formula,[78,142,143]

$$\kappa = \frac{V}{k_B T^2} \int_0^{\infty} \langle Q(t) \cdot Q(t+t') \rangle \, dt' \tag{32}$$

to $\tau_c = L/v$. This choice is reasoned by the fact that lattice waves propagate at speed v until they reach the chain boundaries separated by L, at which point they scatter. The boundary scattering destroys the correlation and sets the correlation decay time determined by the chain length L. Each of these approaches is then aimed at calculating the longtime asymptotic behavior of the heat flux autocorrelation function. These theories predict that the thermal conductivity should diverge as a power law, $\kappa \propto L^{\beta}$. Although the different methods predict similar but different values for β, the common thread among them is that the divergence is attributed to the slow relaxation of long-wavelength modes.

The application of mode coupling theory was pioneered by Lepri and coworkers[126,139,140] and involves projecting the particle displacements onto the normal modes

under the harmonic approximation. The normal mode coordinates are then substituted into the Green–Kubo formula [Eq. (32)], and the limiting behavior for long-wavelength modes can be applied to the original FPU model. The interaction potential in the FPU model is given by[110−112]

$$U = \frac{x^2}{2} + k_3\frac{x^3}{3} + k_4\frac{x^4}{4} \tag{33}$$

where U is the interaction energy; x is the particle separation; and k_3 and k_4 are constants that set the strength of the third- and fourth-order anharmonicity, respectively. For the rate of divergence, Lepri et al.[139,140] obtained β = 1/3 and 1/2 for $k_3 \neq 0$ and k_3 = 0, $k_4 \neq 0$, respectively.

Renormalization group theory was originally proposed by Narayan and Ramaswamy.[141] Their approach considers that when the system is large, long-wavelength modes see the chain as a continuum and thus behave as if in a fluid. By assuming that the only conserved quantities are the total number of particles, total momentum, and energy, they obtained three hydrodynamic equations describing the evolution of the particle density and velocity fields. They then solved the equations and showed that the heat flux autocorrelation decays slowly with β = 1/3.[141]

Peierls originally developed the theory of phonon heat conduction using the Boltzmann equation,[106] where the thermal conductivity is qualitatively given by Eq. (31). Pereverzev[128] used this framework to study the β mode of the FPU model and showed that the relaxation time of long-wavelength modes decayed slowly, $\tau \propto \lambda^{5/3}$. Pereverzev then obtained β = 2/5,[128] which was also later obtained by Lukkarinen and Spohn.[144]

Although each of the approaches has independently predicted/verified a similar rate of divergence, they are all based on the same underlying explanation, which is that some of the long-wavelength modes in a 1D chain of oscillators dissipate their energy very slowly. Another explanation, introduced by Henry and Chen,[108] is based on the possible inapplicability of the Stosszahlansatz assumption in the derivation of the Boltzmann equation.[145] Here, the Stosszahlansatz assumption, originally discussed by Boltzmann,[145] suggests that phonon scattering events are inherently chaotic and uncorrelated. However, the detailed analysis by Henry and Chen[108] shows that for the case of PE chains, the diverging thermal conductivity seems to arise from violation of this assumption. Henry and Chen's analysis is similar to that of Lepri's approach,[139,140] where they used a projection of the particle displacements onto the normal modes and then substituted the normal mode amplitudes into the Green–Kubo expression [Eq. (32)][108]

$$X\left(\mathbf{k}, v, t\right) = \sum_j \sqrt{\frac{m_j}{N}}\mathbf{u}_j\left(t\right) \cdot \mathbf{p}^*\left(\mathbf{k}, v\right) \cdot \exp\left(i\mathbf{k}\mathbf{r}_0\right) \tag{34}$$

where X is the mode amplitude, identified by its wave vector $\mathbf{k}$ and frequency v. The mode amplitude X, can then be used to track the mode total energy E and the deviation from average energy δE, which contains information about the phonon–phonon interactions and is directly proportional to the temporally varying phonon occupation number n

$$E\left(\mathbf{k}, v, t\right) = \frac{1}{2}\omega^2 X \cdot X^* + \frac{1}{2}\dot{X} \cdot \dot{X}^* \tag{35}$$

$$\delta E\left(\mathbf{k},v,t\right)=E\left(\mathbf{k},v,t\right)-\left\langle E\left(\mathbf{k},v,t\right)\right\rangle \tag{36}$$

$$\delta E\left(\mathbf{k},v,t\right)=hv\cdot\delta n\left(\mathbf{k},v,t\right) \tag{37}$$

This then allows us to write the time-dependent heat flux in the system Q as a sum of contributions from individual modes

$$Q\left(t\right)=\frac{1}{V}\sum_{\mathbf{k},v}hv\cdot v\cdot\delta n\left(\mathbf{k},v,t\right) \tag{38}$$

where v represents the phonon group velocity. This expression for the heat flux can then be substituted into the Green–Kubo formula to determine the individual mode contributions to thermal conductivity

$$\kappa=\frac{V}{k_BT^2}\int_0^\infty\left\langle Q\left(t\right)\cdot Q\left(t+t'\right)\right\rangle dt' \tag{39}$$

$$\kappa=\frac{1}{V}\sum_{\mathbf{k},v}\sum_{\mathbf{k}',v'}\sqrt{CC'}\cdot vv'\cdot\int_0^\infty\frac{\left\langle\delta n\left(\mathbf{k},v,t\right)\cdot\delta n\left(\mathbf{k}',v',t+t'\right)\right\rangle}{\sqrt{\left\langle\delta n^2\left(\mathbf{k},v,t\right)\right\rangle\cdot\left\langle\delta n^2\left(\mathbf{k}',v',t\right)\right\rangle}}dt' \tag{40}$$

In this final expression, C is the mode's specific heat, and the individual mode contributions not only include autocorrelations, but also include cross-correlations between different modes. Henry and Chen's approach[108] was able to reveal the extent to which each correlation contributed to the Green–Kubo thermal conductivity integral [Eq. (32)]. Autocorrelations $\mathbf{k}=\mathbf{k}'$ and $v=v'$ indicated that long-wavelength modes do decay slowly, which is in agreement with previous theories. However, the cross-correlations indicated that scattering events between longitudinal modes remain correlated in time and are the primary cause of the divergent thermal conductivity. Of major significance was the fact that the autocorrelations showed long time correlation in all simulations, while the cross-correlations only showed long time correlations in the simulations where the thermal conductivity diverged and showed convergent behavior for convergent simulations. The physical interpretation of these results is simply that divergence in this system is not caused by the long time decay of long-wavelength modes, which implies the lack of phonon–phonon scattering for those modes. Instead, Henry and Chen's results suggest that the divergence is due to correlated/synchronous scattering between select modes in the middle of the Brillouin zone. This explanation offers a different perspective on the issue of anomalous heat conduction, where the divergence can be explained by persistent correlation in the scattering events themselves, rather than the lack of scattering events altogether (ballistic transport).[108]

The prospect of potentially divergent thermal conductivity in polymers opens up interesting possibilities for raising the intrinsic thermal conductivity of polymer-based materials. Experiments on individual chains are needed to verify whether the phenomenon persists in reality or is merely a phenomenon that arises in models. It is also important to study the extent to which this effect can persist in a polymer chain, when it is surrounded by other polymer chains. Studies on groups of PE chains indicate that for PE, the presence of other

chains provides a sufficiently large perturbation that can prevent the correlated scattering events from persisting. For example, Henry and Chen showed that the thermal conductivity of PE chains decreases with increasing dimensionality [(i.e., 1D–two-dimensional (2D) and 2D–three-dimensional (3D) transitions].[146] Liu and Yang have shown that many other polymers may also exhibit high thermal conductivity.[93] Liu and Yang's work has shown that simple monomers, in which the chain axis consists of atoms with homogeneous mass and bond strengths, exhibit the highest thermal conductivities.[93] Their results also suggest that polyphenylene, polybenzimid (PB), and PA can have higher thermal conductivity than PE, due to their stiffer chain backbone and therefore higher phonon velocities.[93] However, more simulations are needed to determine if there are other systems or situations in which the correlation can persist and the thermal conductivity diverges in the limit of an infinitely long chain. Ultimately, the study of single chains provides an upper bound for the performance of groups of interacting molecules because structures involving many chains are presently the most technologically relevant.

It is also important to note that MD simulations[143] of polymers, in general, involve a number of considerations that differ from simulations of other materials. For example, many polymers contain at least one hydrogen atom in the monomer units. Explicit simulation of the motion of hydrogen atoms can have minimal impact on certain properties, such as the glass transition temperature, thermal expansion, or other structural/mechanical properties. Hydrogen atoms are also smaller than all the other elements, which means that their vibrational frequencies are the highest due to their low mass—thus necessitating small sub-femtosecond time steps. Smaller time steps are undesirable because they increase the computational expense required for the same total length of the trajectory. Given these two considerations, it is often a reasonable and computationally advantageous simplification to employ a united-atom approximation. In a united-atom approximation, hydrogen atoms or other degrees of freedom that are unlikely to have an impact on the properties of interest are grouped together with the atoms to which they are bonded in order to form a single rigid degree of freedom. The trajectory of the system of united-atom rigid bodies is then treated with an effective potential. In some cases, this may involve modeling the entire monomer as a single degree of freedom,[147] or portions of the monomer can be treated as a united atom.

Using a united-atom approach can significantly reduce computational time by enabling the use of a larger MD time step for the trajectory. However, for calculations of thermal transport properties, united-atom-based approaches can become problematic.[148] For example, Henry and Chen showed that for MD simulations of PE, including hydrogen atoms as individual degrees of freedom is important to accurately describe the energy carried by certain modes as well as their various interactions. Their work[148] showed that at room temperature, the specific heat of PE, as determined by ab initio calculations and the AIREBO potential, is approximately one-third the value predicted by a united-atom approximation via the model introduced by Kirkwood[147] Henry and Chen[148] also showed that the motion of hydrogen atoms can alter the anharmonicity of the interaction between carbon atoms and that this manifests in significant interactions between low-frequency acoustic phonons and the high-frequency optical phonons that involve the relative motions of hydrogen atoms. As a result, caution should be used in employing united-atom approximations in simulations

of polymer thermal transport properties, such as specific heat, thermal conductivity, or interface resistance.

Another important consideration is that polymers oftentimes involve nearest-neighboring interactions between multiple atomic species. There are a number of potentials available that can treat the species typically found in most polymers, such as REAXFF,[149] AMBER,[150] and CHARMM.[151] Reactive potentials, such as REAXFF and AIREBO[152] involve greater complexity, but offer more realistic depictions of anharmonicity, while simpler potentials such as AMBER and CHARMM are likely to involve less computational time; however, much of the anharmonicity is derived from harmonic terms in the bond angles. Nonetheless, a number of authors have investigated the thermal transport properties of polymers using these potentials; the accuracy of which can be checked through comparison of the thermal conductivity of the amorphous state with experiments. Here, it is important to note that aligned polymers are generally highly anisotropic in nature. Very often, long super-cells with many tens of unit cells along the chain axis are needed for converged results, while for most 3D materials the thermal transport properties converge within less than 10 unit cells in a given direction. Large numbers of unit cells are not necessarily required in the directions perpendicular to the chain axis; however, care should be exercised and convergence, with respect to the number of unit cells, should be checked when studying new systems.[143]

6. THERMAL CONDUCTIVITY OF CRYSTALLINE AND ALIGNED POLYMERS

Most thermal conductivity measurements for crystalline polymers are actually semi-crystalline systems,[79,83,85] in which there are crystalline and amorphous regions. The degree/fraction of crystallinity of the composite system then denotes the relative volumes of these two regions. As such, the composite system thermal conductivity can be described by a modified MG-EMT,[49,79] which takes into account the large degree of anisotropy in a polymer crystal lattice. In a polymer crystal, the polymer chains are packed more densely than in the amorphous phase. In the crystalline phase a single polymer chain traverses one end of the crystal to another and turns around at each edge [see Fig. 8(a)].[1,2] In a region of the polymer where the chains are highly aligned, an entire polymer chain is extended within the length of the region and an array of chains share a common axial orientation, but do not necessarily share common beginning and termination points [see Fig. 8(b)].[1,2] In both the crystalline and aligned polymer regions, there are regions where long sections of individual chains are elongated. In these regions polymer chains can serve as efficient heat conductors along the chain axis due to the stiff covalent bonding. However, in both crystalline and aligned polymer regions individual chains interact with each other through van der Waals forces. This means that real systems consist of arrays of interacting chains, which is a significant departure from the behavior of a single chain.

The experimental data for semi-crystalline polymer systems provides an estimate for the thermal conductivity of the crystalline regions, which is at least an order of magnitude larger in the chain axis direction $\kappa_{||}$ than in perpendicular $\kappa_{\perp}$.[79] As these systems are stretched, a greater degree of chain alignment is achieved and the thermal conductivity

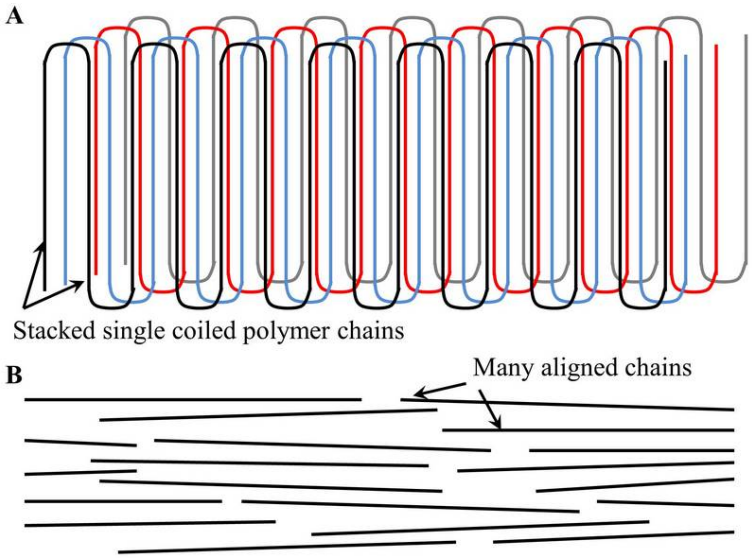

FIG. 8: Illustration of a polymer crystal and aligned polymer. (A) Polymer crystals consist of an array of stacked chains each of which is coiled, forming a #D lattice structure (individual molecules are shown with different colors). (B) Aligned polymers consist of an array of chains that are straightened with a high degree of axial alignment.

increases along the stretching direction and decreases in the perpendicular directions. The decrease in the perpendicular directions can be rationalized by the fact that the amorphous phase is essentially an isotropic mixture of a reduced conductance along the curved/disordered chain backbone and the conductance between chains. In the crystalline polymer the thermal conductivity in the perpendicular direction is only due to conductance between chains, which is slightly lower than the conductance along the curvilinear chain axis.

The thermal conductivity of semi-crystalline and aligned semi-crystalline polymers has been measured by Choy, Chen, and Luk for six different polymers.[49] In their work the thermal conductivity is modeled with an EMT approach,[49] where the MG model is modified to account for anisotropic crystalline regions that are dispersed within the amorphous polymer host. Different degrees of alignment were investigated, by mechanically stretching to different draw ratios (DRs) $\lambda_{DR} = L_f/L_0$, where L_f and L_0 are the initial and final sample lengths, respectively. Their work,[49] showed that a higher DR leads to increased chain alignment and higher thermal conductivity parallel to the stretch direction. In the perpendicular direction, the thermal conductivity decreases because fewer of the chain axes are oriented in those directions. For the amorphous regions, a portion of the heat conduction occurs along the curvilinear chain backbones, and the remainder is transferred between chains through the intermolecular forces. Therefore, as the chain alignment increases, the component of heat conduction in the lateral directions due to vibrations along the chain axes decreases. In the limit of perfect alignment, the only remaining mechanisms for heat conduction in the perpendicular directions are the intermolecular forces. Figure 9 shows the measurements for the samples[49] with the highest stretch ratios for each material. In

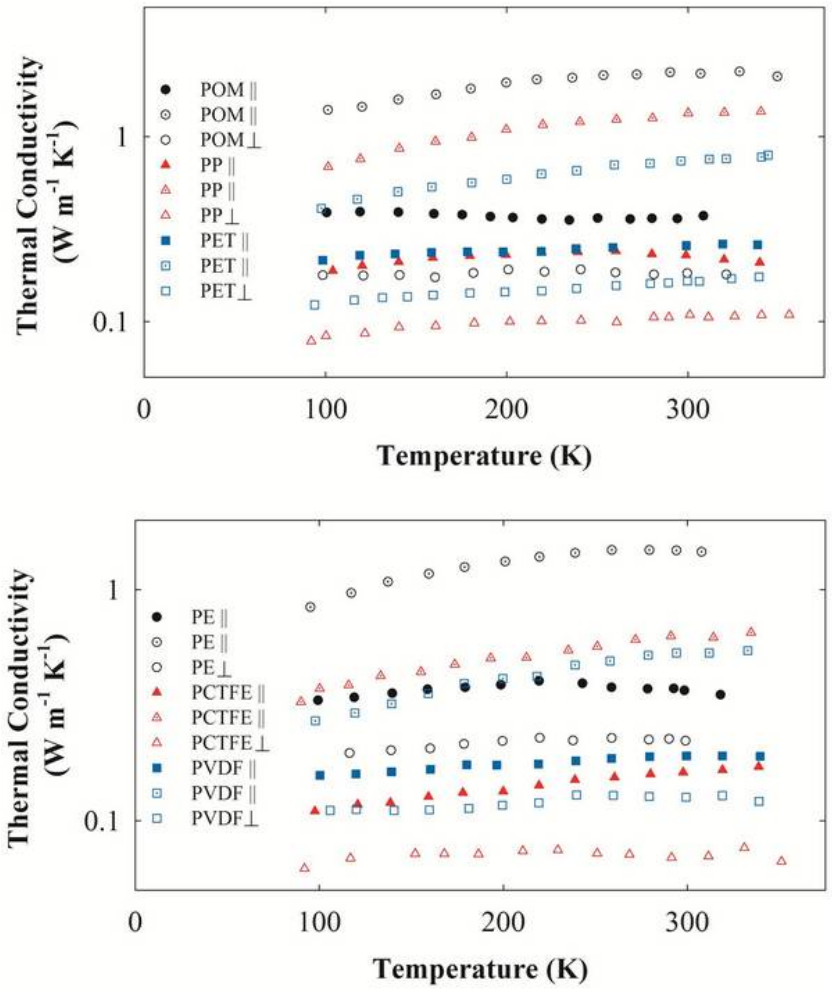

FIG. 9: Thermal conductivity of stretched polymers. The legends indicate whether the thermal conductivity measurement was parallel or perpendicular to the stretching direction for the following six polymers: polyoxymethylene (POM), λ_{DR} = 13; polypropylene (PP), λ_{DR} = 17; polyethylene terephthalate (PET), λ_{DR} = 5; polyethylene (PE), λ_{DR} = 4.2; polychlorotrifluoroethyethylene (PCTFE), λ_{DR} = 4; polyvinylidene fluoride (PVDF), λ_{DR} = 4 (closed symbols correspond to unstretched samples; open symbols correspond to stretched samples).

general, the behavior with respect to temperature is a blend between that of an amorphous material and that of a crystalline material. Both amorphous and crystalline materials exhibit increasing thermal conductivity at low temperatures, which is limited by the specific heat. Amorphous materials have an essentially constant phonon mean-free path and, therefore, exhibit almost constant thermal conductivity up to the glass transition temperature. Typical crystalline materials reach a maximum thermal conductivity, usually bounded by the microstructure where phonon boundary scattering limits the thermal conductivity. Above

the boundary scattering limited peak, the thermal conductivity decreases with increasing temperature as the anharmonicity increases and lowers the mean-free path due to intrinsic phonon–phonon scattering. Choy, Chen, and Luk's measurements of semi-crystalline samples show an increasing thermal conductivity at low temperatures and almost constant κ at moderate temperatures with a slight decrease at higher temperatures that depends on the degree of crystallinity.[49]

To our knowledge, the thermal conductivity of a single polymer crystal or a single region where the chains are highly aligned has never been measured. There are several simulations reported in the literature;[50,146,153] however, the closest measurement to this situation is likely that of Shen et al.,[45] who measured the thermal conductivity of individual ultra-drawn PE nanofibers. Transmission electron microscopy diffraction patterns of these fibers indicated a high degree of alignment, suggesting that the degree of amorphous character is small. However, each highly aligned region is likely connected by slightly amorphous interconnects and arrays of bridging chains. Nonetheless, these fibers exhibited the highest thermal conductivity ever measured for any polymer.[45] Additional experiments are needed to probe the thermal conductivity of individual polymer crystals and individual regions of aligned chains. It may be possible that the thermal conductivity in these regions is substantially higher than what was measured for the individual nanofibers.

7. SUMMARY

Over the last 50 years the usage of polymers has grown tremendously. Polymers can be inexpensive to manufacture, corrosion resistant, and lightweight, all of which are properties that make them attractive for heat transfer applications. Fundamentally, the phonon thermal conductivity of amorphous polymers is limited to $\sim$ 0.1–1.0 W m^{-1} K^{-1}. However, the addition of high thermal conductivity fillers can increase this by approximately 1–2 orders of magnitude. For polymers to compete with other alternatives such as metals, another order of magnitude increase is needed. This could potentially be achieved through alignment of the polymer chains such that each chain becomes a more efficient heat conductor. Mechanical stretching is a potential processing step that can enable higher thermal conductivity; however, an inexpensive high-volume manufacturing process that also results in a material amenable to forming a heat exchanger, heat spreader, or heat sink is still lacking. It is also unclear how much thermal conductivity enhancement can be expected by stretching of polymers other than PE. Simulations indicate that PA, PB, and polypropylene (PP) could exhibit even higher thermal conductivity than PE, with the added benefits of better mechanical properties. With these insights, it will become important to establish enough modeling and experimental results that will allow rational identification or even design of high thermal conductivity polymer molecules. With such advances, inexpensive high thermal conductivity polymer-based materials may enable new functionalities or entirely new applications.

REFERENCES

1. Sperling, L. H., *Introduction to Physical Polymer Science*, Bethelehem, PA: Wiley, 2006.

2. Young, R. J. and Lovell, P. A., *Introduction to Polymers*, Boca Raton, FL: CRC Press, 2011.
3. Friedman, E. M. and Porter, R. S., Polymer viscosity–molecular weight distribution correlations via blending: For high molecular weight poly (dimethyl siloxanes) and for polystyrenes, *Trans. Soc. Rheol.*, vol. 19, pp. 493–508, 1975.
4. Matar, S. and Hatch, L. F., *Chemistry of Petrochemical Processes*, Houston, TX: Gulf Professional Publishing, 2001.
5. Simon, T., Experience curves in the world polymer industry quantifying reductions in production cost, *M.S. Thesis*, Utrecht University, Utrecht, Netherlands, 2009.
6. Tadmor, Z. and Gogos, C. G., *Principles of Polymer Processing*, New York: Wiley, 2006.
7. Wang, X., Yong, Z. Z., Li, Q. W., Bradford, P. D., Liu, W., Tucker, D. S., Cai, W., Wang, H., Yuan, F. G., and Zhu, Y. T., Ultrastrong, stiff and multifunctional carbon nanotube composites, *Mater. Res. Lett.*, vol. 1, no. 1, pp. 19–25, 2013.
8. Spitalsky, Z., Tasis, D., Papagelis, K., and Galiotis, C., Carbon nanotube–polymer composites: Chemistry, processing, mechanical and electrical properties, *Prog. Polym. Sci.*, vol. 35, pp. 357–401, 2010.
9. Han, Z. and Fina, A., Thermal conductivity of carbon nanotubes and their polymer nanocomposites: A review, *Prog. Polym. Sci.*, vol. 36, pp. 914–944, 2011.
10. Moisala, A., Li, Q., Kinloch, I. A., and Windle, A. H., Thermal and electrical conductivity of single- and multi-walled carbon nanotube-epoxy composites, *Compos. Sci. Technol.*, vol. 66, pp. 1285–1288, 2006.
11. Gojny, F. H., Wichmann, M. H. G., Fiedler, B., Kinloch, I. A., Bauhofer, W., Windle, A. H., and Schulte, K., Evaluation and identification of electrical and thermal conduction mechanisms in carbon nanotube/epoxy composites, *Polymer*, vol. 47, pp. 2036–2045, 2006.
12. Breuer, O. and Sundararaj, U., Big returns from small fibers: A review of polymer/carbon nanotube composites, *Polym. Compos.*, vol. 25, pp. 630–645, 2004.
13. Shenogin, S., Xue, L., Ozisik, R., Keblinski, P., and Cahill, D. G., Role of thermal boundary resistance on the heat flow in carbon-nanotube composites, *J. Appl. Phys.*, vol. 95, pp. 8136–8144, 2004.
14. Xu, Y., Ray, G., and Abdel-Magid, B., Thermal behavior of single-walled carbon nanotube polymer–matrix composites, *Composites Part A: Appl. Sci. Manuf.*, vol. 37, pp. 114–121, 2006.
15. Huang, H., Liu, C. H., Wu, Y., and Fan, S., Aligned carbon nanotube composite films for thermal management, *Adv. Mater.*, vol. 17, pp. 1652–1656, 2005.
16. McNally, T., Potschke, P., Halley, P., Murphy, M., Martin, D., Bell, S. E. J., Brennan, G. P., Bein, D., Lemoine, P., and Quinn, J. P., Polyethylene multiwalled carbon nanotube composites, *Polymer*, vol. 46, pp. 8222–8232, 2005.
17. Bagchi, A. and Nomura, S., On the effective thermal conductivity of carbon nanotube reinforced polymer composites, *Compos. Sci. Technol.*, vol. 66, pp. 1703–1712, 2006.
18. Clancy, T. C. and Gates, T. S., Modeling of interfacial modification effects on thermal conductivity of carbon nanotube composites, *Polymer*, vol. 47, pp. 5990–5996, 2006.
19. Berber, S., Kwon, Y.-K., and Tomanek, D., Unusually high thermal conductivity of carbon nanotubes, *Phys. Rev. Lett.*, vol. 84, pp. 4613–4616, 2000.
20. Che, J., Cagin, T., and Goddard III, W. A., Thermal conductivity of carbon nanotubes, *Nan-*

otechnology, vol. 11, pp. 65–69, 2000.

21. Kim, P., Shi, L., Majumdar, A., and McEuen, P. L., Thermal transport measurements of individual multiwalled nanotubes, *Phys. Rev. Lett.*, vol. 87, pp. 215502-1–215502-4, 2001.
22. Lukes, J. and Zhong, H., Thermal conductivity of individual single-wall carbon nanotubes, *J. Heat Transfer*, vol. 129, no. 6, pp. 705–716, 2007.
23. Mingo, N. and Broido, D. A., Length dependence of carbon nanotube thermal conductivity and the "problem of long waves," *Nano Lett.*, vol. 5, pp. 1221–1225, 2005.
24. Moreland, J. F., Freund, J. B., and Chen, G., The disparate thermal conductivity of carbon nanotubes and diamond nanowires studied by atomistic simulation, *Nanoscale Microscale Thermophys. Eng.*, vol. 8, pp. 61–69, 2004.
25. Yu, C., Shi, L., Yao, Z., Li, D., and Majumdar, A., Thermal conductance and thermopower of an individual single-wall carbon nanotube, *Nano Lett.*, vol. 5, pp. 1842–1846, 2005.
26. Yu, A., Ramesh, P., Itkis, M. E., Bekyarova, E., and Haddon, R. C., Graphite nanoplatelet—epoxy composite thermal interface materials, *J. Phys. Chem. C*, vol. 111, pp. 7565–7569, 2007.
27. Agari, Y., Tanaka, M., Nagai, S., and Uno, T., Thermal conductivity of a polymer composite filled with mixtures of particles, *J. Appl. Polym. Sci.*, vol. 34, pp. 1429–1437, 1987.
28. Yu, A., Ramesh, P., Sun, X., Bekyarova, E., Itkis, M. E., and Haddon, R. C., Enhanced thermal conductivity in a hybrid graphite nanoplatelet–carbon nanotube filler for epoxy composites, *Adv. Mater.*, vol. 20, pp. 4740–4744, 2008.
29. Gaier, J. R., YoderVandenberg, Y., Berkebile, S., Stueben, H., and Balagadde, F., The electrical and thermal conductivity of woven pristine and intercalated graphite fiber–polymer composites, *Carbon*, vol. 41, pp. 2187–2193, 2003.
30. Fukushima, H., Drzal, L., Rook, B., and Rich, M., Thermal conductivity of exfoliated graphite nanocomposites, *J. Therm. Anal. Calorim.*, vol. 85, pp. 235–238, 2006.
31. Kalaitzidou, K., Fukushima, H., and Drzal, L. T., Multifunctional polypropylene composites produced by incorporation of exfoliated graphite nanoplatelets, *Carbon*, vol. 45, pp. 1446–1452, 2007.
32. Hung, M. T., Choi, O., Ju, Y. S., and Hahn, H. T., Heat conduction in graphite–nanoplatelet-reinforced polymer nanocomposites, *Appl. Phys. Lett.*, vol. 89, p. 023117, 2006.
33. Mamunya, Y. P., Davydenko, V. V., Pissis, P., and Lebedev, E. V., Electrical and thermal conductivity of polymers filled with metal powders, *Eur. Polym. J.*, vol. 38, pp. 1887–1897, 2002.
34. Bigg, D. M., Mechanical, thermal, and electrical properties of metal fiber-filled polymer composites, *Polym. Eng. Sci.*, vol. 19, pp. 1188–1192, 1979.
35. Tekce, H. S., Kumlutas, D., and Tavman, I. H., Effect of particle shape on thermal conductivity of copper reinforced polymer composites, *J. Reinf. Plast. Compos.*, vol. 26, pp. 113–121, 2007.
36. Wong, C. P. and Bollampally, R. S., Thermal conductivity, elastic modulus, and coefficient of thermal expansion of polymer composites filled with ceramic particles for electronic packaging, *J. Appl. Polym. Sci.*, vol. 74, pp. 3396–3403, 1999.
37. Hill, R. F. and Supancic, P. H., Thermal conductivity of platelet-filled polymer composites, *J. Am. Ceram. Soc.*, vol. 85, pp. 851–857, 2002.

38. Lee, E.-S., Lee, S.-M., Shanefield, D. J., and Cannon, W. R., Enhanced thermal conductivity of polymer matrix composite via high solids loading of aluminum nitride in epoxy resin, *J. Am. Ceram. Soc.*, vol. 91, pp. 1169–1174, 2008.

39. Yu, S., Hing, P., and Hu, X., Thermal conductivity of polystyrene–aluminum nitride composite, *Composites Part A: Appl. Sci. Manuf.*, vol. 33, pp. 289–292, 2002.

40. Ishida, H. and Rimdusit, S., Very high thermal conductivity obtained by boron nitride-filled polybenzoxazine, *Thermochim. Acta*, vol. 320, pp. 177–186, 1998.

41. Pezzotti, G., Kamada, I., and Miki, S., Thermal conductivity of aln/polystyrene interpenetrating networks, *J. Eur. Ceram. Soc.*, vol. 20, pp. 1197–1203, 2000.

42. Kume, S., Yamada, I., Watari, K., Harada, I., and Mitsuishi, K., High-thermal-conductivity AlN filler for polymer/ceramics composites, *J. Am. Ceram. Soc.*, vol. 92, pp. S153–S156, 2009.

43. He, H., Fu, R., Han, Y., Shen, Y., and Song, X., Thermal conductivity of ceramic particle filled polymer composites and theoretical predictions, *J. Mater. Sci.*, vol. 42, pp. 6749–6754, 2007.

44. Xu, Y. and Chung, D. D. L., Increasing the thermal conductivity of boron nitride and aluminum nitride particle epoxy-matrix composites by particle surface treatments, *Compos. Interfaces*, vol. 7, pp. 243–256, 2000.

45. Shen, S., Henry, A., Tong, J., Zheng, R., and Chen, G., Polyethylene nanofibres with very high thermal conductivities, *Nat. Nanotechnol.*, vol. 5, pp. 251–255, 2010.

46. Choy, C. L., Wong, Y. W., Yang, G. W., and Kanamoto, T., Elastic modulus and thermal conductivity of ultradrawn polyethylene, *J. Polym. Sci., Part B: Polym. Phys.*, vol. 37, pp. 3359–3367, 1999.

47. Huang, X. and Jiang, P., A review of dielectric polymer composites with high thermal conductivity, *IEEE Electr. Insul. Mag.*, vol. 27, pp. 8–16, 2011.

48. Choy, C. L., Luk, W. H., and Chen, F. C., Thermal conductivity of highly oriented polyethylene, *Polymer*, vol. 19, pp. 155–162, 1978.

49. Choy, C. L., Chen, F. C., and Luk, W. H., Thermal conductivity of oriented crystalline polymers, *J. Polym. Sci., Polym. Phys. Ed.*, vol. 18, pp. 1187–1207, 1980.

50. Choy, C. L., Wong, S. P., and Young, K., Model calculation of the thermal conductivity of polymer crystals, *J. Polym. Sci., Polym. Phys. Ed.*, vol. 23, pp. 1495–1504, 1985.

51. Gibson, A. G., Greig, D., Sahota, M., Ward, I. M., and Choy, C. L., Thermal conductivity of ultrahigh-modulus polyethylene, *J. Polym. Sci., Polym. Lett. Ed.*, vol. 15, pp. 183–192, 1977.

52. Choy, C. L., Fei, Y., and Xi, T. G., Thermal conductivity of gel-spun polyethylene fibers, *J. Polym. Sci., Part B: Polym. Phys.*, vol. 31, pp. 365–370, 1993.

53. Cevallos, J. G., Bergles, A. E., Bar-Cohen, A., Rodgers, P., and Gupta, S. K., Polymer heat exchangers—History, opportunities, and challenges, *Heat Transfer Eng.*, vol. 33, pp. 1075–1093, 2012.

54. Githens, R. E., Minor, W. R., and Tomsic, V. J., Flexible tube heat exchangers (properties of small tube Teflon heat exchangers noting corrosion resistance, smooth slippery surface, etc., and heat transfer coefficient), *Chem. Eng. Prog.*, vol. 61, pp. 55–62, 1965.

55. Pescod, D., A heat exchanger for energy saving in an air-conditioning plant, *ASHRAE Trans.*, vol. 85, pp. 238–251, 1979.

56. Pescod, D., Shah, R. K., McDonald, C. F., and Howard, C. P., An advance in plate heat exchanger geometry giving increased heat transfer, *Proc. of ASME Winter Annual Meeting*, Chicago, IL, 1980.

57. Pescod, D., Unit air cooler using plastic heat exchanger with evaporatively cooled plates, *Aust. Refrig. Air Cond. Heat.*, vol. 22, pp. 22–26, 1968.

58. Miller, D., Holtz, R. E., Koopman, R. N., Marciniak, T. J., and D. R. MacFarlane, Plastic heat exchangers: State-of-the-art review, *Report ANL 79-12*, Lemont, IL: Argonne National Laboratory, 1979.

59. Reay, D. A., The use of polymers in heat exchangers, *Heat Recovery Syst. CHP*, vol. 9, pp. 209–216, 1989.

60. Luckow, P., Bar-Cohen, A., and Rodgers, P., Minimum mass polymer seawater heat exchanger for LNG applications, *J. Thermal Sci. Eng. Appl.*, vol. 1, pp. 031009–031010, 2009.

61. Agari, Y., Ueda, A., and Nagai, S., Thermal conductivity of a polyethylene filled with disoriented short-cut carbon fibers, *J. Appl. Polym. Sci.*, vol. 43, pp. 1117–1124, 1991.

62. Kuriger, R. J., Alam, M. K., Anderson, D. P., and Jacobsen, R. L., Processing and characterization of aligned vapor grown carbon fiber reinforced polypropylene, *Composites Part A: Appl. Sci. Manuf.*, vol. 33, pp. 53–62, 2002.

63. Tibbetts, G. G., Lake, M. L., Strong, K. L., and Rice, B. P., A review of the fabrication and properties of vapor-grown carbon nanofiber/polymer composites, *Compos. Sci. Technol.*, vol. 67, pp. 1709–1718, 2007.

64. Al-Saleh, M. H. and Sundararaj, U., A review of vapor grown carbon nanofiber/polymer conductive composites, *Carbon*, vol. 47, pp. 2–22, 2009.

65. Nielsen, L. E., The thermal and electrical conductivity of two-phase systems, *Ind. Eng. Chem. Fundam.*, vol. 13, pp. 17–20, 1974.

66. Sieder, E. N., Plastic heat exchangers for sea solar plants, *Proc. of 2nd Ocean Thermal Energy Workshop*, pp. 149–158, 1975.

67. Suratt, W. B., Hart, G. K., and Sieder, E. N., Development of plastic heat exchangers for sea solar power plants, *NTIS Technical Report 7518*, Washington, DC: National Aeronautics and Space Administration, 1975.

68. Hart, G. K., Lee, C. O., and Latour, S. R., Development of plastic heat exchangers for ocean thermal energy conversion, *Final Report*, Ft. Lauderdale, FL: DSS Engineers, Inc., 1979.

69. McGowan, J. G., Ocean thermal energy conversion—A significant solar resource, *Sol. Energy*, vol. 18, pp. 81–92, 1976.

70. Bar-Cohen, A., Rodgers, P., and Cevallos, J. G., Application of thermally enhanced thermoplastics to seawater-cooled liquid–liquid heat exchangers, *Proc. of 5th European Thermal Sciences Conference*, 2008.

71. Sadasivam, S., Che, Y., Huang, Z., Chen, L., Kumar, S., and Fisher, T. S., The Atomistic Green's function method for interfacial phonon transport, *Ann. Rev. Heat Transfer*, vol. 17, pp. 89–145, 2014.

72. Chalopin, Y., Rajabpour, A., Han, H., Ni, Y., and Volz, S., Equilibrium molecular dynamics simulations on interfacial phonon transport, *Ann. Rev. Heat Transfer*, vol. 17, pp. 147–176, 2014.

73. Prasher, R., Thermal interface materials: Historical perspective, status, and future directions,

Proc. IEEE, vol. 94, pp. 1571–1586, 2006.

74. Garimella, S. V., Fleischer, A. S., Murthy, J. Y., Keshavarzi, A., Prasher, R., Patel, C., Bhavnani, S. H., Venkatasubramanian, R., Mahajan, R., and Joshi, Y., Thermal challenges in next-generation electronic systems, *IEEE Trans. Compon. Packag. Technol.*, vol. 31, pp. 801–815, 2008.
75. Wang, R. Y., Segalman, R. A., and Majumdar, A., Room temperature thermal conductance of alkanedithiol self-assembled monolayers, *Appl. Phys. Lett.*, vol. 89, pp. 173113-1–173113-3, 2006.
76. Wang, Z., Carter, J. A., Lagutchev, A., Koh, Y. K., Seong, N.-H., Cahill, D. G., and Dlott, D. D., Ultrafast flash thermal conductance of molecular chains, *Science*, vol. 317, pp. 787–789, 2007.
77. Srivastava, G. P., *Physics of Phonons*, New York: Adam Hilger, 1990.
78. Chen, G., *Nanoscale Energy Transport and Conversion: A Parallel Treatment of Electrons, Molecules, Phonons, and Photons*, New York: Oxford University Press, 2005.
79. Choy, C. L., Thermal conductivity of polymers, *Polymer*, vol. 18, pp. 984–1004, 1977.
80. Klemens, P. G., The thermal conductivity of dielectric solids at low temperatures (theoretical), *Proc. R. Soc. London. Ser. A: Math. Phys. Sci.*, vol. 208, pp. 108–133, 1951.
81. Pomeranchuk, I., On the thermal conductivity of dielectrics, *Phys. Rev.*, vol. 60, pp. 820–821, 1941.
82. Landau, L. and Rumer, G., Absorption of sound in solids, *Phys. Z. Sowjetunion*, vol. 11, pp. 18–25, 1937.
83. Kline, D. E. and Hansen, D., *Techniques and Methods of Polymer Evaluation*, Slade, P. E. and Jenkins, L. T., eds., vol. 2, pp. 247–292, 1970.
84. Morikawa, J., Tan, J., and Hashimoto, T., Study of change in thermal diffusivity of amorphous polymers during glass transition, *Polymer*, vol. 36, pp. 4439–4443, 1995.
85. Anderson, D. R., Thermal conductivity of polymers, *Chem. Rev.*, vol. 66, pp. 677–690, 1966.
86. Ueberreiter, K. and Otto-Laupenmuhlen, E., Spezifische warme, spezifisches volumen, temperatur-und warmeleitfahigkeit von hocholymeren, Teil II. Kettenlangenabhangigkeit bei fraktionierten polystyrolen, *Z. Naturforsch. Teil A*, vol. 8, p. 664, 1953.
87. Hansen, D. and Ho, C. C., Thermal conductivity of high polymers, *J. Polym. Sci., Part A: Gen. Pap.*, vol. 3, pp. 659–670, 1965.
88. Hansen, D., Kantayya, R. C., and Ho, C. C., Thermal conductivity of high polymers—The influence of molecular weight, *Polym. Eng. Sci.*, vol. 6, pp. 260–262, 1966.
89. Tomlinson, J. N., Kline, D. E., and Sauer, J. A., Effect of nuclear radiation on the thermal conductivity of polyethylene, *Polym. Eng. Sci.*, vol. 5, pp. 44–48, 1965.
90. Hennig, J., Knappe, W., and Lohe, P., Die warmeleitfahigkeit von polyathylen im temperaturbereich von 20 bis 200°C, *Kolloid Z. Z. Polym.*, vol. 189, pp. 114–116, 1963.
91. Nolas, G. S., Cohn, J. L., Slack, G. A., and Schujman, S. B., Semiconducting Ge clathrates: Promising candidates for thermoelectric applications, *Appl. Phys. Lett.*, vol. 73, pp. 178–180, 1998.
92. Sales, B. C., Chakoumakos, B. C., Mandrus, D., and Sharp, J. W., Atomic displacement parameters and the lattice thermal conductivity of clathrate-like thermoelectric compounds, *J.*

Solid State Chem., vol. 146, pp. 528–532, 1999.

93. Liu, J. and Yang, R., Length-dependent thermal conductivity of single extended polymer chains, *Phys. Rev. B*, vol. 86, pp. 104307-1–104307-8, 2012.
94. Klemens, P. G., Thermal resistance due to point defects at high temperatures, *Phys. Rev.*, vol. 119, pp. 507–509, 1960.
95. Jeng, M.-S., Yang, R., Song, D., and Chen, G., Modeling the thermal conductivity and phonon transport in nanoparticle composites using Monte Carlo simulation, *J. Heat Transfer*, vol. 130, pp. 042410–042411, 2008.
96. Progelhof, R. C., Throne, J. L., and Ruetsch, R. R., Methods for predicting the thermal conductivity of composite systems: A review, *Polym. Eng. Sci.*, vol. 16, pp. 615–625, 1976.
97. Nan, C.-W., Birringer, R., Clarke, D. R., and Gleiter, H., Effective thermal conductivity of particulate composites with interfacial thermal resistance, *J. Appl. Phys.*, vol. 81, pp. 6692–6699, 1997.
98. Garnett, J. C. M., Colours in metal glasses and in metallic films, *Proc. R. Soc. London*, vol. 73, pp. 443–445, 1904.
99. Donea, J., Thermal conductivities based on variational principles, *J. Compos. Mater.*, vol. 6, pp. 262–266, 1972.
100. Hamilton, R. L. and Crosser, O. K., Thermal conductivity of heterogeneous two-component systems, *Ind. Eng. Chem. Fundam.*, vol. 1, pp. 187–191, 1962.
101. Lin, W., Zhang, R., and Wong, C. P., Modeling of thermal conductivity of graphite nanosheet composites, *J. Electron. Mater.*, vol. 39, pp. 268–272, 2010.
102. Coleman, J. N., Curran, S., Dalton, A. B., Davey, A. P., McCarthy, B., Blau, W., and Barklie, R. C., Percolation-dominated conductivity in a conjugated-polymer–carbon-nanotube composite, *Phys. Rev. B*, vol. 58, pp. 7492–7495, 1998.
103. Berber, S., Kwon, Y.-K., and Tomanek, D., Unusually high thermal conductivity of carbon nanotubes, *Phys. Rev. Lett.*, vol. 84, pp. 4613–4616, 2000.
104. Olson, J. R., Pohl, R. O., Vandersande, J. W., Zoltan, A., Anthony, T. R., and Banholzer, W. F., Thermal conductivity of diamond between 170 and 1200 K and the isotope effect, *Phys. Rev. B*, vol. 47, pp. 14850–14856, 1993.
105. Balandin, A. A., Ghosh, S., Bao, W., Calizo, I., Teweldebrhan, D., Miao, F., and Lau, C. N., Superior thermal conductivity of single-layer graphene, *Nano Lett.*, vol. 8, pp. 902–907, 2008.
106. Peierls, R., Zur kinetischen theorie der warmeleitung in kristallen, *Ann. Phys.*, vol. 395, pp. 1055–1101, 1929.
107. Henry, A. and Chen, G., High thermal conductivity of single polyethylene chains using molecular dynamics simulations, *Phys. Rev. Lett.*, vol. 101, no. 23, pp. 235502-1–235502-4, 2008.
108. Henry, A. and Chen, G., Anomalous heat conduction in polyethylene chains: Theory and molecular dynamics simulations, *Phys. Rev. B*, vol. 79, no. 14, pp. 144305-1–144305-10, 2009.
109. Lee, W., Song, B., and Reddy, P., Measurement of thermoelectric and thermal transport properties of single-molecule junctions, *Ann. Rev. Heat Transfer*, vol. 16, pp. 259–286, 2013.
110. Fermi, E., Pasta, J., and Ulam, S., Studies of nonlinear problems, *Report LA-1940*, Los Alamos, NM: Los Alamos Laboratory, 1955.

111. Berman, G. P. and Izraileva, F. M., The Fermi–Pasta–Ulam problem: Fifty years of progress, *Chaos*, vol. 15, no. 1, pp. 015104-1–015104-18, 2005.

112. Campbell, D. K., Rosenau, P., and Zaslavsky, G. M., Introduction: The Fermi–Pasta–Ulam problem—The first fifty years, *Chaos*, vol. 15, no. 1, pp. 015101-1–015101-4, 2005.

113. Liu, S., Xu, X., Xie, R., Zhang, G., and Li, B., Anomalous heat conduction and anomalous diffusion in low dimensional nanoscale systems, *Eur. Phys. J. B*, vol. 85, no. 10, pp. 1–20, 2012.

114. Li, B. and Wang, J., Anomalous heat conduction and anomalous diffusion in one-dimensional systems, *Phys. Rev. Lett.*, vol. 91, no. 4, pp. 44301-1–44301-4, 2003.

115. Li, N., Tong, P., and Li, B., Effective phonons in anharmonic lattices: Anomalous vs. normal heat conduction, *Europhys. Lett.*, vol. 75, no. 1, pp. 49–55, 2006.

116. Li, N. and Li, B., Temperature dependence of thermal conductivity in 1D nonlinear lattices, *Europhys. Lett.*, vol. 78, no. 3, pp. 1–6, 2007.

117. Liu, Z. and Li, B., Heat conduction in a one-dimensional harmonic chain with three-dimensional vibrations, *J. Phys. Soc. Jpn.*, vol. 77, pp. 074003-1–074003-4, 2008.

118. Casati, G. and Li, B., Heat conduction in one dimensional systems: Fourier Law, Chaos, and Heat Control, *Non-Linear Dynamics and Fundamental Interactions*, F. Khanna and D. Matrasulov, eds., pp. 1–16, Dordrecht, Netherlands: Springer, 2006.

119. Lepri, S., Livi, R., and Politi, A., On the anomalous thermal conductivity of one-dimensional lattices, *Europhys. Lett.*, vol. 43, no. 3, pp. 271–276, 1998.

120. Lepri, S., Livi, R., and Politi, A., Universality of anomalous one-dimensional heat conductivity, *Phys. Rev. E*, vol. 68, no. 6, pp. 067102-1–067102-4, 2003.

121. Livi, R. and Lepri, S., Heat in one dimension, *Nature*, vol. 421, p. 327, 2003.

122. Delfini, L., Lepri, S., Livi, R., and Politi, A., Anomalous kinetics and transport from 1D self-consistent mode-coupling theory, *J. Stat. Mech.: Theory Exp.*, vol. 2007, p. 02007, 2007.

123. Lepri, S., Mejia-Monasterio, C., and Politi, A., A stochastic model of anomalous heat transport: Analytical solution of the steady state, *J. Phys. A: Math. Theor.*, vol. 42, p. 025001, 2008.

124. Basile, G., Delfini, L., Lepri, S., Livi, R., Olla, S., and Politi, A., Anomalous transport and relaxation in classical one-dimensional models, *Eur. Phys. J. Spec. Top.*, vol. 151, pp. 85–93, 2007.

125. Prosen, T. and Campbell, D. K., Momentum Conservation implies anomalous energy transport in 1D classical lattices, *Phys. Rev. Lett.*, vol. 84, pp. 2857–2860, 2000.

126. Delfini, L., Lepri, S., Livi, R., and Politi, A., Self-consistent mode-coupling approach to one-dimensional heat transport, *Phys. Rev. E*, vol. 73, no. 6, pp. 060201-1–060201-4, 2006.

127. Prosen, T. and Campbell, D. K., Normal and anomalous heat transport in one-dimensional classical lattices, *Chaos*, vol. 15, no. 1, pp. 015117-1–015117-17, 2005.

128. Pereverzev, A., Fermi–Pasta–Ulam β lattice: Peierls equation and anomalous heat conductivity, *Phys. Rev. E*, vol. 68, no. 5, pp. 056124-1–056124-6, 2003.

129. Shiba, H. and Ito, N., Anomalous heat conduction in three-dimensional nonlinear lattices, *J. Phys. Soc. Jpn.*, vol. 77, pp. 054006-1–054006-8, 2008.

130. van Beijeren, H., Exact results for anomalous transport in one-dimensional Hamiltonian sys-

tems, *Phys. Rev. Lett.*, vol. 108, no. 18, pp. 180601-1–180601-5, 2012.

131. Lepri, S., Livi, R., and Politi, A., Studies of thermal conductivity in Fermi–Pasta–Ulam-like lattices, *Chaos*, vol. 15, pp. 015118–015119, 2005.
132. Zhang, G. and Li, B., Thermal conductivity of nanotubes revisited: Effects of chirality, isotope impurity, tube length, and temperature, *J. Chem. Phys.*, vol. 123, p. 114714, 2005.
133. Pan, R.-Q., Xu, Z.-J., and Zhu, Z.-Y., Length dependence of thermal conductivity of single-walled carbon nanotubes, *Chin. Phys. Lett.*, vol. 24, no. 5, p. 1321, 2007.
134. Maruyama, S., A Molecular dynamics simulation of heat conduction in finite length SWNTs, *Physica B: Condens. Matter*, vol. 323, pp. 193–195, 2002.
135. Maruyama, S., A molecular dynamics simulation of heat conduction of a finite length single-walled carbon nanotube, *Microscale Thermophys. Eng.*, vol. 7, pp. 41–50, 2003.
136. Lukes, J. R. and Zhong, H., Thermal conductivity of individual single-wall carbon nanotubes, *J. Heat Transfer*, vol. 129, pp. 705–716, 2007.
137. Lepri, S., Livi, R., and Politi, A., Studies of thermal conductivity in Fermi–Pasta–Ulam-like lattices, *Chaos*, vol. 15, no. 1, pp. 015118-1–015118-9, 2005.
138. Liu, S., Xu, X. F., Xie, R. G., Zhang, G., and Li, B. W., Anomalous heat conduction and anomalous diffusion in low dimensional nanoscale systems, *Eur. Phys. J. B*, vol. 85, pp. 1–20, 2012.
139. Lepri, S., Livi, R., and Politi, A., On the anomalous thermal conductivity of one-dimensional lattices, *Europhys. Lett.*, vol. 43, pp. 271–276, 1998.
140. Lepri, S., Relaxation of classical many-body Hamiltonians in one dimension, *Phys. Rev. E*, vol. 58, no. 6, pp. 7165–7171, 1998.
141. Narayan, O. and Ramaswamy, S., Anomalous heat conduction in one-dimensional momentum-conserving systems, *Phys. Rev. Lett.*, vol. 89, no. 20, pp. 200601-1–200601-4, 2002.
142. Hansen, J. and McDonald, I., *Theory of Simple Liquids*, London: Academic Press, 1986.
143. McGaughey, A. J. H. and Larkin, J. M., Predicting phonon properties from equilibrium molecular dynamics simulations, *Ann. Rev. Heat Transfer*, vol. 17, pp. 49–87, 2014.
144. Aoki, K., Lukkarinen, J., and Spohn, H., Energy transport in weakly anharmonic chains, *J. Stat. Phys.*, vol. 124, pp. 1105–1129, 2006.
145. Cercignani, C., *Theory and Application of the Boltzmann Equation*, New York: Elsevier, 1975.
146. Henry, A., Chen, G., Plimpton, S. J., and Thompson, A., 1D-to-3D transition of phonon heat conduction in polyethylene using molecular dynamics simulations, *Phys. Rev. B*, vol. 82, no. 14, pp. 144308-1–144308-5, 2010.
147. Kirkwood, J., The skeletal modes of vibration of long chain molecules, *J. Chem. Phys.*, vol. 7, pp. 506–509, 1939.
148. Henry, A. S. and Chen, G., Explicit treatment of hydrogen atoms in thermal simulations of polyethylene, *Nanoscale Microscale Thermophys. Eng.*, vol. 13, no. 2, pp. 99–108, 2009.
149. van Duin, A. C. T., Dasgupta, S., Lorant, F., and Goddard, W. A., ReaxFF: A reactive force field for hydrocarbons, *J. Phys. Chem. A*, vol. 105, pp. 9396–9409, 2001.
150. Salomon-Ferrer, R., Case, D. A., and Walker, R. C., An overview of the Amber biomolecular simulation package, *Wiley Interdiscip. Rev.: Comput. Mol. Sci.*, vol. 3, no. 2, pp. 198–210,

2012.

151. Brooks, B. R., Bruccoleri, R. E., Olafson, B. D., States, D. J., Swaminathan, S., and Karplus, M., CHARMM: A program for macromolecular energy, minimization, and dynamics calculations, *J. Comput. Chem.*, vol. 4, pp. 187–217, 1983.
152. Stuart, S. J., Tutein, A. B., and Harrison, J. A., A reactive potential for hydrocarbons with intermolecular interactions, *J. Chem. Phys.*, vol. 112, pp. 6472–6486, 2000.
153. Rossinsky, E. and Muller-Plathe, F., Anisotropy of the thermal conductivity in a crystalline polymer: Reverse nonequilibrium molecular dynamics simulation of the delta phase of syndiotactic polystyrene, *J. Chem. Phys.*, vol. 130, pp. 134905–134909, 2009.